Journal of Quality Measurement and Analysis *JQMA* 22(1) 2026, 173-204
e-ISSN: 2600-8602 *http://www.ukm.my/jqma*
https://doi.org/10.17576/jqma.2201.2026.10

PERFORMANCE OF THE DOUBLE SAMPLING COEFFICIENT OF VARIATION CHART UNDER MEASUREMENT ERRORS USING A LINEAR COVARIATE ERROR MODEL FOR MONITORING NPK FERTILIZER MANUFACTURING PROCESS

(*Prestasi Carta Pensampelan Berganda Dua Pekali Variasi di Bawah Ralat Pengukuran Menggunakan Model Ralat Kovariat Linear untuk Pemantauan Proses Pembuatan Baja NPK*)

MUHAMMAD ALIFIAN NURIMAN, MICHAEL B.C. KHOO*, SAJAL SAHA, ZHI LIN CHONG & SHANYU CHUA

ABSTRACT

The double sampling (DS) coefficient of variation (CV) chart has been investigated in the literature under the assumption that the quality characteristic of interest is measured with no measurement error (ME). However, in practical applications, measurement errors caused by gauge equipment are often unavoidable and can lead to inconsistent process monitoring. In this manuscript, the performance of DS CV chart with measurement errors, referred to as the DS CV - ME chart is studied. The linear covariate error model, based on the constant error variance and that based on the error variance which is a linearly increasing function of the mean, is utilized. The DS CV - ME chart is evaluated using the average number of observations to signal (ANOS) and expected ANOS (EANOS) performance metric. The findings demonstrate that measurement errors diminish the DS CV - ME chart's detection ability. Using a larger value of the coefficient B of the linear covariate error model can ameliorate the DS CV - ME chart's performance. Additionally, the findings show that taking multiple measurements per item does not notably reduce the negative effect of measurement errors. A real-world application in manufacturing is provided to showcase the DS CV - ME chart's working.

Keywords: DS CV - ME chart; measurement errors; linear covariate error; constant error variance; error variance which is a linearly increasing function of the mean; manufacturing process

ABSTRAK

Carta pekali variasi (CV) pensampelan berganda dua (DS) telah dikaji dalam literatur dengan andaian bahawa ciri kualiti yang diminati diukur tanpa ralat pengukuran (ME). Walau bagaimanapun, ralat pengukuran yang disebabkan oleh peralatan tolok sering tidak dapat dielakkan dalam aplikasi praktikal dan boleh membawa kepada pemantauan proses yang tidak konsisten. Dalam manuskrip ini, prestasi carta pensampelan berganda dua (DS) pekali variasi (CV) dengan ralat pengukuran (ME), yang dirujuk sebagai carta DS CV - ME dikaji kerana ralat pengukuran tidak dapat dielakkan dalam amalan. Model ralat kovariat linear berdasarkan varians ralat malar dan yang berdasarkan varians ralat yang merupakan fungsi meningkat secara linear min digunakan. Carta DS CV - ME dinilai menggunakan metrik prestasi purata bilangan cerapan untuk berisyarat (ANOS) dan ANOS jangkaan (EANOS). Penemuan menunjukkan bahawa ralat pengukuran mengurangkan keupayaan pengesanan carta DS - CV ME. Penggunaan nilai yang lebih besar bagi pekali *B* dalam model ralat kovariat linear boleh memperbaiki prestasi carta DS CV - ME. Tambahan pula, penemuan menunjukkan bahawa pengambilan beberapa pengukuran bagi setiap item tidak mengurangkan kesan negatif ralat pengukuran dengan ketara. Suatu aplikasi dunia sebenar dalam pembuatan diberikan untuk menunjukkan cara kerja carta DS CV - ME.

Kata kunci: carta DS CV - ME; ralat pengukuran; ralat kovariat linear; varians ralat malar; varians ralat yang merupakan fungsi meningkat secara linear min; proses pembuatan

1. Introduction

Control charts are often designed for process monitoring by assuming that the process mean and standard deviation remain constant when the process is in-control (Teoh *et al.* (2014); Santhanasamy & Abdul-Rahman (2022); Mehmood *et al*. (2023); Saadatmellia *et al*. (2023); Haq *et al*. (2024); Saha *et al*. (2024); Teoh *et al*. (2025a); Shafie *et al.* (2025); Chong *et al.* (2025)). However, in many process settings, such as in the agricultural sector (Whelen & Siqueira 2018), biological sciences (Pélabon *et al*. 2020), economy (Jin *et al*. 2022) and pharmaceutical (Diaz-Tufinio *et al*. 2024), it was found that the process mean is not stable and/or the standard deviation changes with the mean. For these types of processes, the coefficient of variation (CV) chart is the most appropriate chart for implementation (Lim *et al*. 2024).

Kang *et al*. (2007) proposed the first CV chart, which is the Shewhart CV chart. Hong *et al*. (2008) developed a two- sided exponentially weighted moving average (EWMA) CV chart to improve the Shewhart CV chart by Kang *et al*. (2007). Castagliola *et al*. (2011) suggested a one-sided EWMA CV - γ^2 chart that has higher efficiency than the two-sided EWMA CV chart of Hong *et al*. (2008). Calzada and Scariano (2013) suggested a synthetic CV chart which beats the basic Shewhart CV chart of Kang *et al*. (2007) even though the said chart falls behind the EWMA CV - γ^2 chart of Castagliola *et al*. (2011) in identifying small shifts. Subsequently, Zhang *et al*. (2014) developed a modified EWMA CV chart to improve the EWMA CV - γ^2 chart of Castagliola *et al*. (2011).

Some researchers have explored adaptive types of Shewhart CV charts, where the charts' parameters are adjusted based on information from previous samples. These adaptive charts include the variable sampling interval CV charts of Castagliola *et al*. (2013) and Lau *et al*. (2018), the variable sample size (VSS) CV charts by Castagliola *et al*. (2015) and Yeong *et al*. (2017a), and the variable sample size and sampling interval CV charts by Khaw *et al*. (2017). Yeong *et al*. (2018) showed that the variable parameters (VP) CV charts have the best performance among all adaptive Shewhart CV charts. More recently, Lee *et al*. (2021) improved the detection ability of the VP CV chart of Yeong *et al*. (2018) by developing the double sampling (DS) CV chart, which involves taking a second sample should the information obtained from the first sample is not enough to determine the process CV condition. The DS CV chart of Lee *et al*. (2021) was found to be superior to the VP CV chart of Yeong *et al*. (2018) in detecting small and large CV shifts but the EWMA CV - γ^2 chart prevails over the DS CV chart in identifying small shifts.

The research works discussed above did not consider the impact of measurement errors on control charts even though such errors are unavoidable in process monitoring. Linna and Woodall (2001) initiated the linear covariate error model to assess how measurement errors affect the Shewhart chart. Hu *et al*. (2015, 2016) used the same linear covariate error model as that used by Linna and Woodall (2001) to study how measurement errors affect the synthetic $\overline{X}$ and VSS $\overline{X}$ charts. Moreover, numerous researchers, such as Cheng and Wang (2018a, 2018b), Tran *et al*. (2019b), Nguyen and Tran (2020), Nguyen *et al*. (2020), Hassani *et al*. (2021), Abubakar *et al*. (2022), Mim *et al*. (2023), Munir *et al*. (2023), Sharafi *et al*. (2024) and Xie *et al*. (2024) have studied how measurement errors affect various types of control charts. However, their studies assumed that the variance of the errors is constant. Linna and Woodall (2001), Montgomery and Runger (1993), Maravelakis *et al*. (2004), Haq *et al*.

(2015) and Haizhen *et al*. (2025) claimed that in some cases, such as in automotive assembly, the variance of the errors is dependent on the process mean.

The effect of measurement errors on the Shewhart CV chart was first studied by Yeong *et al*. (2017b). Subsequently, Tran *et al*. (2019a) studied how the precision $\left(\sigma_M/\sigma_0\right)$ and accuracy $\left(A/\mu_0\right)$ errors affect the performance of the Shewhart CV chart. They demonstrated that the precision and accuracy errors substantially impacted the Shewhart CV chart. Other researchers have also studied how measurement errors affect CV charts, for example, see Nguyen *et al*. (2019), Lee *et al*. (2020), Saha *et al*. (2021) and Arshad *et al*. (2024). It should be noted that these researchers only assumed that the measurement errors have a constant error variance. As far as the authors are aware, investigations on the effect of measurement errors on CV charts using the linear covariate error model when the error variance is a linearly increasing function of the mean, has yet to be investigated in the literature.

In the literature, the DS CV chart has significantly improved the sensitivity of the basic and adaptive Shewhart CV charts, such as the VP CV chart, in identifying small and large shifts in the CV. However, the existing DS CV chart was developed under the assumption that the quality characteristic being monitored is devoid of measurement errors although such errors are inevitable in process monitoring. Therefore, it is more realistic to take into account the presence of measurement errors in the design and evaluation of the DS CV chart.

This paper aims at investigating how measurement errors affect the DS CV chart by using the linear covariate error model, for both the constant error variance and an error variance which is a linearly increasing function of the mean. Integrating the linear covariate error model into the DS CV chart is valuable for process CV monitoring when the gauge system (e.g., tapes, calipers and weight gauge) produces observed values that deviate from the quality characteristic of interest. In other words, the quality characteristic of interest may be correlated through the covariate (i.e., gauge system) with an observed value. The derivations of the average number of observations to signal (ANOS) and expected average number of observations to signal (EANOS) formulae are provided, for evaluating the performance of the DS CV chart with measurement errors, referred to as DS CV - ME chart.

The main contribution and significance of this study lies in its practical value for monitoring the process CV in industries. By integrating measurement errors, the proposed DS CV - ME chart provides a process monitoring approach that better mirrors real production settings, where the measurement systems are never perfectly accurate. This enhances the reliability in detecting process variation and contributes to more consistent product quality and informed process control decisions.

The remainder of this paper is structured as follows: In Section 2, the linear covariate error models are elaborated. The sample CV with the linear covariate error model is presented in Section 3. Section 4 provides the statistics and charting procedures for the DS CV - ME chart. The performance criteria and optimal designs of the DS CV - ME chart are discussed in Sections 5 and 6, respectively. The DS CV - ME chart's performance is studied in Section 7. Section 8 illustrates how the DS CV - ME chart is implemented based on a real-world NPK fertilizer manufacturing process. Section 9 concludes the paper and provides recommendations for future research directions.

2. Linear Covariate Error Models

Linna and Woodall (2001) assumed that the quality characteristic *X*, for observation *j* (= 1, 2,…, *n*) in sample *i*, i.e., X_{ij}, where *n* (≥ 1) is the sample size, is not directly observable but it can be assessed from $\left\{X^*_{ij1}, X^*_{ij2}, ..., X^*_{ijm}\right\}$, with X^*_{ijk} representing the k^{th} measurement of an item, for *k* = 1, 2, …, *m* and *m* ≥ 1. The variables X_{ij} are assumed to be independent and identically distributed having the normal distribution with the mean $\mu_0 + a\sigma_0$ and standard deviation $b\sigma_0$. Consequently, X^*_{ijk} can be represented by means of the linear covariate error model as

$$X^*_{ijk} = A + BX_{ij} + \varepsilon_{ijk}, \tag{1}$$

where A and B are the intercept and slope of the measurement error model, respectively, while ε_{ijk} is the random error term. Note that there are $m \times n$ observations of X^*_{ijk}. The mean of the observable quality characteristics $\{X^*_{ij1}, X^*_{ij2}, ..., X^*_{ijm}\}$ is

$$\bar{X}^*_{ij} = \frac{1}{m}\sum_{k=1}^{m} X^*_{ijk} = A + BX_{ij} + \frac{1}{m}\sum_{k=1}^{m}\varepsilon_{ijk}. \tag{2}$$

Sections 2.1 and 2.2 consider the CV of $\bar{X}^*_{ij}$ with a constant error variance and an error variance which is a linearly increasing function of the mean, respectively.

2.1. *Linear covariate error model with a constant error variance*

Linna and Woodall (2001) assumed that the variance of the error, ε_{ijk}, in Eq. (1) is constant and has the normal distribution, i.e., $\varepsilon_{ijk} \sim N(0, \sigma^2_M)$. Also, ε_{ijk} is independent of X_{ij}. The mean and standard deviation of $\bar{X}^*_{ij}$ in Eq. (2), based on a constant variance of the error term is computed as

$$\mu^* = A + B(\mu_0 + a\sigma_0) \tag{3}$$

and

$$\sigma^* = \sqrt{B^2 b^2 \sigma_0^2 + \frac{\sigma_M^2}{m}}, \tag{4}$$

respectively. Let $\eta = \sigma_M / \sigma_0$ and $\theta = A/\mu_0$. Also, the in-control CV for the process without measurement error is $\gamma_0 = \sigma_0/\mu_0$. Consequently, when measurement errors exist, the CV of $\bar{X}^*_{ij}$ in Eq. (2) is obtained as

$$\gamma^* = \frac{\sqrt{B^2 b^2 \sigma_0^2 + \frac{\sigma_M^2}{m}}}{A + B(\mu_0 + a\sigma_0)} = \frac{\sqrt{\frac{B^2 b^2 \sigma_0^2}{\mu_0^2} + \frac{\eta^2\sigma_0^2 / \mu_0^2}{m}}}{\frac{A}{\mu_0} + B\left(\frac{\mu_0 + a\sigma_0}{\mu_0}\right)}$$

$$= \frac{\gamma_0\sqrt{B^2 b^2 + \frac{\eta^2}{m}}}{\theta + B(1 + a\gamma_0)}. \tag{5}$$

In Eq. (5), η is the precision error ratio, θ is the accuracy error and γ_0 is the in-control CV. Letting a = 0 and b = 1 in Eq. (5) gives the in-control CV when measurement errors exist as follows:

$$\gamma_0^* = \frac{\gamma_0\sqrt{B^2 + \frac{\eta^2}{m}}}{\theta + B}. \tag{6}$$

In addition, for the process without measurement error, the out-of-control CV is obtained as $\gamma_+ = \delta\gamma_0 = b\sigma_0/(\mu_0 + a\sigma_0) = b\gamma_0/(1 + a\gamma_0)$. From this relation, the following equation is obtained:

$$1 + a\gamma_0 = \frac{b}{\delta}. \tag{7}$$

Based on Eqs. (5) and (7), the out-of-control CV of $\bar{X}_{ij}^*$ when measurement errors are present can be obtained as

$$\gamma_+^* = \frac{\gamma_0\sqrt{B^2b^2 + \frac{\eta^2}{m}}}{\theta + \frac{Bb}{\delta}}, \tag{8}$$

where $\delta \neq 1$. Note that when $\theta = 0$, $\eta = 0$ and $B = 1$, the out-of-control CV (γ_+^*) in Eq. (8) under the constant variance of the error term for the linear covariate error model in Eq. (1) becomes the out-of-control CV (γ_+) without measurement error. Moreover, it should also be noted that when $\delta = 1$, γ_+^* and γ_+ reduce to their respective in-control CVs of γ_0^* and γ_0, respectively.

2.2. *Linear covariate error model with an error variance which is a linearly increasing function of the mean*

In some practical situations, the variance of the measurement errors in Eq. (1) should be considered as a linearly increasing function of the mean of X_{ij},, i.e., $\sigma_M^2 = C + D(\mu_0 + a\sigma_0)$, where C and D are both constants. Under this condition, the measurement errors follow a normal distribution, given as $\varepsilon_{ijk} \sim N(0, C + D(\mu_0 + a\sigma_0))$ (Linna and Woodall 2001; Maravelakis *et al*. 2004; Haq *et al*. 2015; Haizhen *et al*. 2025). It follows that the mean and standard deviation of $\bar{X}_{ij}^*$ in Eq. (2) becomes

$$\mu^* = A + B(\mu_0 + a\sigma_0) \tag{9}$$

and

$$\sigma^* = \sqrt{B^2b^2\sigma_0^2 + \frac{C + D\,(\mu_0 + a\sigma_0)}{m}}. \tag{10}$$

From Eqs. (9) and (10), the CV of $\bar{X}_{ij}^*$ when measurement errors exist, is obtained and given in Eq. (11).

$$\gamma^* = \frac{\sqrt{B^2b^2\sigma_0^2 + \frac{C + D(\mu_0 + a\sigma_0)}{m}}}{A + B(\mu_0 + a\sigma_0)}. \tag{11}$$

Also, let $\theta = A/\mu_0$, $\omega = \sqrt{C}/\sigma_0$ and $\phi = \sqrt{D\mu_0}/\sigma_0$. Then Eq. (11) can be rewritten as

$$\gamma^* = \frac{\sqrt{\dfrac{B^2 b^2 \sigma_0^2}{\mu_0^2} + \dfrac{\omega^2 \sigma_0^2}{\mu_0^2 m} + \dfrac{D\left(\mu_0 + a\sigma_0\right)}{\mu_0^2 m}}}{\dfrac{A + B\left(\mu_0 + a\sigma_0\right)}{\mu_0}} = \frac{\gamma_0 \sqrt{B^2 b^2 + \dfrac{\omega^2}{m} + \dfrac{\phi^2\left(1 + a\gamma_0\right)}{m}}}{\theta + B\left(1 + a\gamma_0\right)}. \tag{12}$$

Appendix 1 shows how the term on the right-hand side of Eq. (12) is obtained.

Letting a = 0 and b = 1 in Eq. (12), the in-control CV of $\bar{X}_{ij}^*$ when measurement errors exist is computed as

$$\gamma_0^* = \frac{\gamma_0 \sqrt{B^2 + \dfrac{\omega^2 + \phi^2}{m}}}{\theta + B}. \tag{13}$$

Meanwhile, based on Eqs. (7) and (12), the out-of-control CV of $\bar{X}_{ij}^*$ when measurement errors exist is computed as

$$\gamma_+^* = \frac{\gamma_0 \sqrt{B^2 b^2 + \dfrac{\omega^2 + \phi^2 \left(b/\delta\right)}{m}}}{\theta + \dfrac{Bb}{\delta}}. \tag{14}$$

Here, θ denotes the accuracy error, while ω and ϕ are components of the precision error, and γ_0 is the in-control CV. It is observed that if θ = 0, ω = 0, ϕ = 0 and B = 1, the out-of-control CV in Eq. (14) under the linear increasing variance of the linear covariate error model in Eq. (1) reduces to the out-of-control CV without measurement errors, i.e., γ_+.

3. Sample CV with the Linear Covariate Error Model

Let $\bar{\bar{X}}_i^*$ and S_i^* be the sample mean and sample standard deviation of $\left\{\bar{X}_{i1}^*, \bar{X}_{i2}^*, \ldots, \bar{X}_{in}^*\right\}$. Then

$$\bar{\bar{X}}_i^* = \frac{\sum_{j=1}^{n} \bar{X}_{ij}^*}{n} \tag{15}$$

and

$$S_i^* = \sqrt{\frac{1}{n-1} \sum_{j=1}^{n} \left(\bar{X}_{ij}^* - \bar{\bar{X}}_i^*\right)^2}. \tag{16}$$

Based on Eqs. (15) and (16), the sample CV with the linear covariate error model is computed as

$$\hat{\gamma}_i^* = \frac{S_i^*}{\bar{\bar{X}}_i^*}. \tag{17}$$

In this article, the approximations of the cumulative distribution functions (cdfs) of the sample CV and sample CV squared by Tran *et al*. (2019a) in Eqs. (18) and (19), respectively, are adopted:

$$F_{\hat{\gamma}^*}\left(x \mid n, \gamma^*\right) \simeq 1 - F_t\left(\frac{\sqrt{n}}{x} \mid n-1, \frac{\sqrt{n}}{\gamma^*}\right), \tag{18}$$

where $F_t(\ \cdot\ )$ is the cdf of the non-central t distribution, $n - 1$ is the degree of freedom and $\sqrt{n}/\gamma^*$ is the non-centrality parameter, while

$$F_{\hat{\gamma}^{*2}}\left(x \mid n, \gamma^*\right) = 1 - F_F\left(\frac{n}{x} \mid 1, n-1, \frac{n}{\gamma^{*2}}\right), \tag{19}$$

where $F_F(\ \cdot\ )$ is the cdf of the non-central F distribution, 1 and $n - 1$ are the degrees of freedom, and n/γ^{*2} is the non-centrality parameter.

4. DS CV - ME Chart

The linear covariate error models with the (i) constant error variance and (ii) error variance which is a linearly increasing function of the mean, discussed in Sections 2.1 and 2.2, respectively, are used to evaluate the DS CV - ME chart. The operating procedure of the DS CV - ME chart is given henceforth. Figure 1 shows the DS CV - ME chart.

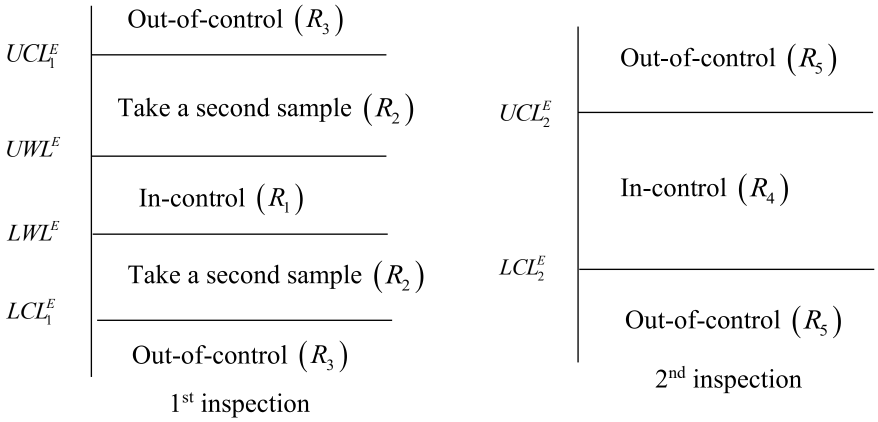

Figure 1: A graphical procedure of the DS CV – ME chart

The control and warning limits of the DS CV - ME chart can be calculated as follows:

$$UCL_l^E = \mu_0\left(\hat{\gamma}^* \mid \sum_{t=1}^{l} n_t\right) + ku_l^E \times \sigma_0\left(\hat{\gamma}^* \mid \sum_{t=1}^{l} n_t\right), \tag{20a}$$

$$LCL_l^E = \mu_0\left(\hat{\gamma}^* \mid \sum_{t=1}^{l} n_t\right) - kl_l^E \times \sigma_0\left(\hat{\gamma}^* \mid \sum_{t=1}^{l} n_t\right), \tag{20b}$$

$$UWL^E = \mu_0\left(\hat{\gamma}^* \mid n_1\right) + wu^E \times \sigma_0\left(\hat{\gamma}^* \mid n_1\right), \tag{20c}$$

and

$$LWL^{E} = \mu_0\left(\hat{\gamma}^* \mid n_1\right) - wl^{E} \times \sigma_0\left(\hat{\gamma}^* \mid n_1\right), \tag{20d}$$

where l = 1 or 2 refers to the 1st or 2nd inspection, respectively. The mean and standard deviation of $\hat{\gamma}^*$ can be obtained from the formulae provided in Hong *et al*. (2008) by replacing γ_0 with γ_0^* defined in Eq. (6) for the linear covariate error model with a constant error variance, and Eq. (13) for the linear covariate error model with an error variance which is a linearly increasing function of the mean. It follows that the mean and standard deviation of $\hat{\gamma}^*$ are

$$\mu_0\left(\hat{\gamma}^* \mid \sum_{t=1}^{l} n_t\right) \simeq \gamma_0^* \left[\begin{array}{l} 1 + \dfrac{1}{\sum_{t=1}^{l} n_t}\left(\gamma_0^{*2} - \dfrac{1}{4}\right) + \dfrac{1}{\left(\sum_{t=1}^{l} n_t\right)^2}\left(3\gamma_0^{*4} - \dfrac{\gamma_0^{*2}}{4} - \dfrac{7}{32}\right) \\ + \dfrac{1}{\left(\sum_{t=1}^{l} n_t\right)^3}\left(15\gamma_0^{*6} - \dfrac{3\gamma_0^{*4}}{4} - \dfrac{7\gamma_0^{*2}}{32} - \dfrac{19}{128}\right) \end{array}\right] \tag{21}$$

and

$$\sigma_0\left(\hat{\gamma}^* \mid \sum_{t=1}^{l} n_t\right) \simeq \gamma_0^* \left[\begin{array}{l} 1 + \dfrac{1}{\sum_{t=1}^{l} n_t}\left(\gamma_0^{*2} + \dfrac{1}{2}\right) + \dfrac{1}{\left(\sum_{t=1}^{l} n_t\right)^2}\left(8\gamma_0^{*4} - \gamma_0^{*2} - \dfrac{3}{8}\right) \\ + \dfrac{1}{\left(\sum_{t=1}^{l} n_t\right)^3}\left(69\gamma_0^{*6} + \dfrac{7\gamma_0^{*4}}{2} + \dfrac{3\gamma_0^{*2}}{4} + \dfrac{3}{16}\right) \end{array}\right]^{1/2}. \tag{22}$$

The DS CV - ME chart's statistic at inspection level 1 of sampling stage i is $\hat{\gamma}_{1i}^* = \dfrac{S_{1i}^*}{\bar{\bar{X}}_{1i}^*}$, where $\bar{\bar{X}}_{1i}^* = \dfrac{\sum_{j=1}^{n_1} \bar{X}_{1ij}^*}{n_1}$ and $S_{1i}^* = \sqrt{\dfrac{\sum_{j=1}^{n_1}\left(\bar{X}_{1ij}^* - \bar{\bar{X}}_{1i}^*\right)^2}{n_1 - 1}}$. At inspection level 2 of sampling stage i, the combined first and second sample CVs is calculated as $\hat{\gamma}_i^{**} = \sqrt{\dfrac{(n_1-1)\hat{\gamma}_{1i}^{*2} + (n_2-1)\hat{\gamma}_{2i}^{*2}}{(n_1-1)+(n_2-1)}}$, where $\hat{\gamma}_{2i}^* = \dfrac{S_{2i}^*}{\bar{\bar{X}}_{2i}^*}$, $S_{2i}^* = \sqrt{\dfrac{\sum_{j=1}^{n_2}\left(\bar{X}_{2ij}^* - \bar{\bar{X}}_{2i}^*\right)^2}{n_2 - 1}}$ and $\bar{\bar{X}}_{2i}^* = \dfrac{\sum_{j=1}^{n_2} \bar{X}_{2ij}^*}{n_2}$. By referring to Figure 1, the DS CV - ME chart can be implemented using the following steps:

1. Determine the parameters (i) $n_1, n_2, ku_1^E, kl_1^E, wu^E, wl^E, ku_2^E, kl_2^E, m, B, \theta$ and η for the linear covariate error model with a constant error variance, and (ii) $n_1, n_2, ku_1^E, kl_1^E, wu^E$, $wl^E, ku_2^E, kl_2^E, m, B, \theta, \omega$ and ϕ for the linear covariate error model with an error variance which is a linearly increasing function of the mean.
2. Compute the control and warning limits using Eqs. (20a) - (20d), based on the parameters determined in step 1.

3. Draw a sample of size n_1 at inspection level 1 of sampling stage *i*, then calculate $\bar{\bar{X}}^*_{1i}$, S^*_{1i} and $\hat{\gamma}^*_{1i} = \frac{S^*_{1i}}{\bar{\bar{X}}^*_{1i}}$.
4. If $\hat{\gamma}^*_{1i} \in R_1$,, the process is in-control. Then return to step 3.
5. If $\hat{\gamma}^*_{1i} \in R_3$, the process is out-of-control. Then move to step 10.
6. If $\hat{\gamma}^*_{1i} \in R_2$, draw a second sample of size n_2 at inspection level 2 of sampling stage *i*. Then calculate $\bar{\bar{X}}^*_{2i}$, S^*_{2i} and $\hat{\gamma}^*_{2i} = \frac{S^*_{2i}}{\bar{\bar{X}}^*_{2i}}$.
7. Compute the combined first and second sample CVs, $\hat{\gamma}^{**}_i = \sqrt{\frac{(n_1-1)\hat{\gamma}^{*2}_{1i} + (n_2-1)\hat{\gamma}^{*2}_{2i}}{(n_1-1)+(n_2-1)}}$.
8. If $\hat{\gamma}^{**}_i \in R_4$, the process is in-control. Then go back to step 3.
9. If $\hat{\gamma}^{**}_i \in R_5$, the process is out-of-control. Then advance to step 10.
10. An out-of-control is issued at sampling stage *i* and corrective actions should be performed.
11. Remove the assignable cause(s) and go back to step 3.

5. Derivation of Out-of-Control Probabilities and Performance Measures

This section provides the derivations of out-of-control probabilities and performance measures of the DS CV - ME chart.

5.1. *Out-of-control probabilities*

Let P^E_{ooc} denotes the probability that a sampling stage is out-of-control and $P^E_{\text{ooc}l}$ represents the probability that a process is out-of-control at inspection level *l* (=1 or 2) of the said sampling stage. Thus,

$$P^E_{\text{ooc}} = P^E_{\text{ooc1}} + P^E_{\text{ooc2}}. \tag{23}$$

The probability that a sampling stage becomes out-of-control at inspection level 1 is

$$P^E_{\text{ooc1}} = P\left(\hat{\gamma}^*_1 \in R_3 \mid \gamma^*_+\right) = 1 - F_t\left(\frac{\sqrt{n_1}}{LCL^E_1} \mid n_1 - 1, \frac{\sqrt{n_1}}{\gamma^*_+}\right) + F_t\left(\frac{\sqrt{n_1}}{UCL^E_1} \mid n_1 - 1, \frac{\sqrt{n_1}}{\gamma^*_+}\right). \tag{24}$$

Meanwhile, the probability of a sampling stage becoming out-of-control at inspection level 2 is

$$P^E_{\text{ooc2}} = P\left(\hat{\gamma}^*_1 \in R_2 \cap \hat{\gamma}^{**} \in R_5 \mid \gamma^*_+\right). \tag{25}$$

where

$$P\left(\hat{\gamma}^*_1 \in R_2 \mid \gamma^*_+\right) = P\left(LCL^E_1 \le \hat{\gamma}^*_1 \le LWL^E \mid n_1, \gamma^*_+\right) + P\left(UWL^E \le \hat{\gamma}^*_1 \le UCL^E_1 \mid n_1, \gamma^*_+\right)$$

$$= \int_{\frac{\sqrt{n_1}}{LWL^E}}^{\frac{\sqrt{n_1}}{LCL_1^E}} f_t\left(u_1^* \mid n_1 - 1, \frac{\sqrt{n_1}}{\gamma_+^*}\right) du_1^* + \int_{\frac{\sqrt{n_1}}{UCL_1^E}}^{\frac{\sqrt{n_1}}{UWL^E}} f_t\left(u_1^* \mid n_1 - 1, \frac{\sqrt{n_1}}{\gamma_+^*}\right) du_1^* \quad (26)$$

and

$$P\left(\hat{\gamma}^{**} \in R_5 \mid n_1 + n_2, \gamma_+^*\right) = F_F\left(\frac{n_2}{UCL_2^{E*}} \mid 1, n_2 - 1, \frac{n_2}{\gamma_+^{*2}}\right) + \left[1 - F_F\left(\frac{n_2}{LCL_2^{E*}} \mid 1, n_2 - 1, \frac{n_2}{\gamma_+^{*2}}\right)\right], \quad (27)$$

where $UCL_2^{E*} = \left(\frac{n_1 - 1}{n_2 - 1} + 1\right)\left(UCL_2^E\right)^2 - \frac{(n_1 - 1)n_1}{(n_2 - 1)u_1^{*2}}$, $LCL_2^{E*} = \left(\frac{n_1 - 1}{n_2 - 1} + 1\right)\left(LCL_2^E\right)^2 - \frac{(n_1 - 1)n_1}{(n_2 - 1)u_1^{*2}}$ and $u_1^* = \sqrt{n_1}/\hat{\gamma}_1^*$. Castagliola *et al*. (2013) showed that u_1^* has a noncentral *t* distribution with $n_1 - 1$ degrees of freedom and a non-centrality parameter $\sqrt{n_1}/\gamma_+^*$ (see Appendix 3). Based on Eqs. (26) and (27), Eq. (25) can be written as

$$\begin{aligned} P_{\text{ooc}2}^E &= P\left(\hat{\gamma}_1^* \in R_2 \cap \hat{\gamma}^{**} \in R_5 \mid \gamma_+^*\right) \\ &= \int_{\frac{\sqrt{n_1}}{LWL^E}}^{\frac{\sqrt{n_1}}{LCL_1^E}} \left[F_F\left(\frac{n_2}{UCL_2^{E*}} \mid 1, n_2 - 1, \frac{n_2}{\gamma_+^{*2}}\right) + \left[1 - F_F\left(\frac{n_2}{LCL_2^{E*}} \mid 1, n_2 - 1, \frac{n_2}{\gamma_+^{*2}}\right)\right]\right] \times f_t\left(u_1^* \mid n_1 - 1, \frac{\sqrt{n_1}}{\gamma_+^*}\right) du_1^* \\ &+ \int_{\frac{\sqrt{n_1}}{UCL_1^E}}^{\frac{\sqrt{n_1}}{UWL^E}} \left[F_F\left(\frac{n_2}{UCL_2^{E*}} \mid 1, n_2 - 1, \frac{n_2}{\gamma_+^{*2}}\right) + \left[1 - F_F\left(\frac{n_2}{LCL_2^{E*}} \mid 1, n_2 - 1, \frac{n_2}{\gamma_+^{*2}}\right)\right]\right] \times f_t\left(u_1^* \mid n_1 - 1, \frac{\sqrt{n_1}}{\gamma_+^*}\right) du_1^*. \quad (28) \end{aligned}$$

Appendix 2 shows how the term on the right-hand side of Eq. (24) is obtained, while Appendices 3 and 4 show how the term on the right-hand side of Eqs. (26) and (27), respectively are obtained. Note that γ_+^* in Eq. (8) is adopted when the variance of the errors is constant, while γ_+^* in Eq. (14) is used when the variance of the errors is a function that increases with the mean.

5.2. *Performance measures*

A control chart's efficiency is determined by assessing the speed it detects a process shift. Following Lee *et al*. (2021), the average run length (ARL) of the DS CV - ME chart for the shift size in the process CV (δ) is computed as $\text{ARL}(\delta) = \frac{1}{P_{\text{ooc}}^{\text{E}}}$, where P_{ooc}^E is obtained from Eq. (23). However, the ANOS criterion carries more weight because the DS CV - ME chart requires varying number of observations at each sampling stage (Teoh *et al*. 2025b), i.e., either n_1 or $n_1 + n_2$. The ANOS of the DS CV - ME chart for the shift δ can be obtained as

$$\text{ANOS}(\delta) = \text{ARL}(\delta) \times \text{ASS}(\delta), \quad (29)$$

where ASS(δ) represents the average sample size of the DS CV - ME chart which is computed as

$$\text{ASS}(\delta)=n_1+n_2\,P\left(\hat{\gamma}_1^*\in R_2\,|\,\gamma_+^*\right)$$

$$=n_1+n_2\left[\int_{\frac{\sqrt{n_1}}{LWL^E}}^{\frac{\sqrt{n_1}}{LCL_1^E}} f_t\left(u_1^*\,|\,n_1-1,\frac{\sqrt{n_1}}{\gamma_1^*}\right)du_1^*+\int_{\frac{\sqrt{n_1}}{UCL_1^E}}^{\frac{\sqrt{n_1}}{UWL^E}} f_t\left(u_1^*\,|\,n_1-1,\frac{\sqrt{n_1}}{\gamma_1^*}\right)du_1^*\right] \tag{30}$$

and the derivation of $P\left(\hat{\gamma}_1^*\in R_2\,|\,\gamma_+^*\right)$ is given in Appendix 3. When the exact shift δ is unknown, the EANOS metric should be employed, instead of the ANOS (Saha *et al*. 2026). The EANOS value of the DS CV - ME chart, for shifts in the interval $\left(\delta_{\min},\delta_{\max}\right)$ is computed using the following equation:

$$\text{EANOS}\left(\delta_{\min},\delta_{\max}\right)=\int_{\delta_{\min}}^{\delta_{\max}}\text{ANOS}(\delta)\,f(\delta)\,\mathrm{d}\delta\,. \tag{31}$$

In Eq. (31), $f(\delta)$ is the probability density function of the shift size δ. If information about $f(\delta)$ is unavailable, Sparks (2000) and Wu *et al*. (2008) suggested using the assumption that δ has a uniform, $U\left(\delta_{\min},\delta_{\max}\right)$ distribution.

6. Optimization Models of the DS CV – ME Chart

This section elucidates two different optimization models for the DS CV - ME chart. The combination of charting parameters must satisfy $2<n_1<n_0<n_2\le n_{\max}$, $0<wu^E<ku_1^E$, $0<wl^E<kl_1^E$, $0<ku_2^E<ku_1^E$ and $0<kl_2^E<kl_1^E$ in computing the limits $UWL^E<UCL_1^E$, $LCL_1^E<LWL^E$, $UCL_2^E<UCL_1^E$, and $LCL_1^E<LCL_2^E$. In most applications, the value of $n_{\max}$ is typically set as 31 due to the limited number of items in a sample (Castagliola *et al*. 2013; Castagliola *et al*. 2015; Khaw *et al*. 2017; Yeong *et al*. 2018). All the computations in this paper are made using the MATLAB 2023a software. Additionally, to verify the accuracy of the MATLAB 2023a computations, verifications are made using simulations conducted in the SAS program.

6.1. *ANOS based optimization*

The optimization model by minimizing ANOS(δ) in Eq. (29), for $\delta>1$, is explained henceforth.

$$\underset{n_1,n_2,ku_1^E,kl_1^E,wu^E,wl^E,ku_2^E,kl_2^E}{\text{Minimize}}\quad \text{ANOS}(\delta), \tag{32}$$

subject to the constraints ANOS($\delta=1$) = τ_1, ASS($\delta=1$) = n_0, and the specified values (i) m, B, θ and η for the linear covariate error model with a constant error variance, (ii) m, B, θ, ω and ϕ for the linear covariate error model with an error variance which is a linearly increasing function of the mean. Note that τ_1 and n_0 are the desirable values of ANOS and ASS when the CV is in-control. In this study, a nonlinear constraint solver method (see Lee 2013 and Lee *et al*. 2021) is adopted to obtain the optimal parameters of the DS CV - ME chart. The step-by-step approach below explains how the optimal parameters of the DS CV - ME chart that minimize ANOS(δ), for $\delta>1$, are computed.

Step 1. Set τ_1, n_0, γ_0 and δ (> 1) values, and that of (i) *m, B, θ* and *η* for the linear covariate error model with a constant error variance, (ii) *m, B, θ, ω* and *ϕ* for the linear covariate error model with an error variance which is a linearly increasing function of the mean. Also, let $\text{ANOS}_{\min} = \infty$.

Step 2. Determine a possible (n_1, n_2) combination that satisfies the constraint $2 < n_1 < n_2 \leq 31$. If no further (n_1, n_2) combination is available, proceed to step 5.

Step 3. Utilize a nonlinear constraint solver (provided in the MATLAB toolbox) to obtain the parameters $n_1, n_2, ku_1^E, kl_1^E, wu^E, wl^E, ku_2^E$ and kl_2^E that satisfy the parameter values specified in step 1 and (n_1, n_2) combination in step 2, followed by computing the corresponding ANOS(δ) value for the value of δ (> 1) specified in step 1.

Step 4. If ANOS(δ) < $\text{ANOS}_{\min}$, for the δ (> 1) value specified in step 1, let $\text{ANOS}_{\min}$ = ANOS(δ). Here, the smallest value of ANOS(δ) is recorded as $\text{ANOS}_{\min}$. Then, go back to step 2.

Step 5. The parameters $n_1, n_2, ku_1^E, kl_1^E, wu^E, wl^E, ku_2^E$ and kl_2^E, which results in the computation of the smallest ANOS(δ) (= $\text{ANOS}_{\min}$) value are taken as the optimal parameters.

Figure 2 shows a flowchart for the optimization algorithm of the DS CV - ME chart in minimizing ANOS(δ), for $\delta > 1$. In this analysis, we set τ_1 = 1,852, n_0 = 5, $m \in \{1, 3, 5, 7\}$, $B \in \{1, 2, 3, 4\}$, $\theta \in \{0, 0.01, 0.03, 0.05\}$, $\eta \in \{0, 0.1, 0.3, 0.5\}$, $\omega \in \{0, 0.1, 0.2, 0.3\}$, $\phi \in \{0, 0.1, 0.2, 0.3\}$, $\delta \in \{1.01, 1.05, 1.1, 1.3, 1.5, 2\}$ and γ_0 = 0.05.

6.2. *EANOS based optimization*

The optimization model for the DS CV - ME chart which minimizes the out-of-control EANOS is given below:

$$\underset{n_1, n_2, ku_1^E, kl_1^E, wu^E, wl^E, ku_2^E, kl_2^E}{\text{Minimize}} \quad \text{EANOS}(\delta_{\min}, \delta_{\max}), \tag{33}$$

subject to the constraints EANOS(δ = 1) = ANOS(δ = 1) = τ_1, ASS(δ = 1) = n_0, and the specified values (i) *m*, *B*, *θ* and *η* for the linear covariate error model with a constant error variance, (ii) *m, B, θ, ω* and *ϕ* for the linear covariate error model with an error variance which is a linearly increasing function of the mean. In this section, the values of *m, B, θ, η*, *ω* and *ϕ* are set to be the same as that in Section 6.1. The steps in Section 6.1 and the flowchart for the optimization algorithm in Figure 2 can also be employed in obtaining the optimal parameters $n_1, n_2, ku_1^E, kl_1^E, wu^E, wl^E, ku_2^E, kl_2^E$ that minimize EANOS $(\delta_{\min}, \delta_{\max})$ but by changing $\text{ANOS}_{\min}$ to $\text{EANOS}_{\min}$, ANOS(δ) to EANOS$(\delta_{\min}, \delta_{\max})$ and Eq. (29) to Eq. (31).

7. Assessment of the DS CV – ME Chart's Performance

This section provides the performance evaluation of the DS CV - ME chart based on the linear covariate error model with the (i) constant error variance and (ii) error variance which is a linearly increasing function of the mean. Without loss of generality, this study assumes that $b = 1$, i.e. similar to the assumption made by Tran *et al*. (2019a).

7.1. *Performance of the DS CV – ME chart with a constant error variance*

Table 1 illustrates the optimal parameters and corresponding ANOS(δ) values, for various θ, η, m and B values when δ is specified. Different values of $\theta \in \{0, 0.01, 0.03, 0.05\}$, for fixed values of η (= 0.28), m (= 1), B (= 1), γ_0 (= 0.05) and n_0 (= 5), are considered. Note that η = 0.28 is an acceptable signal-to-ratio value which was reported in Tran *et al*. (2019a).

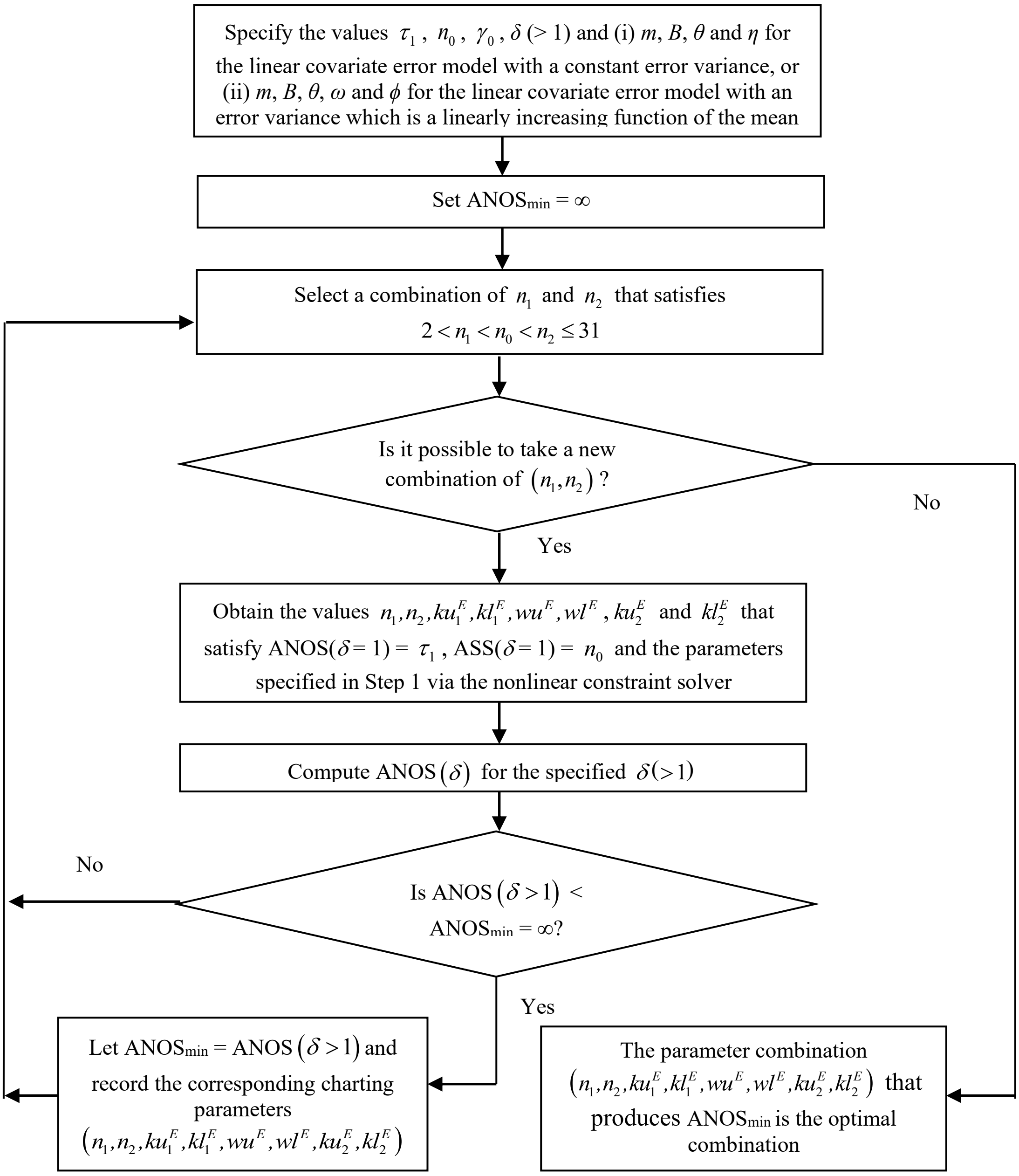

Figure 2: A flowchart for the optimization algorithm of the DS CV - ME chart in minimizing ANOS(δ)

It can be seen that θ affects the DS CV - ME chart's performance negatively, as ANOS(δ), for $\delta > 1$ increases with θ. For instance, when $\delta = 1.05$, ANOS(1.05) $\in$ {712.79, 718.96, 731.49, 743.65} for $\theta \in \{0, 0.01, 0.03, 0.05\}$, respectively (see Table 1). Table 1 shows that η has a negligible effect on the DS CV - ME chart's performance, as ANOS(δ) does not change much when η changes, For instance, when $\theta = 0$, $m = B = 1$, $\gamma_0 = 0.05$, $n_0 = 5$ and $\delta = 2$, ANOS(2) $\in$ {21.20, 21.20, 21.20, 21.21} for $\eta \in \{0, 0.1, 0.3, 0.5\}$, where the value of ANOS(2) does not change much when η changes. According to Lee *et al*. (2020) and Saha *et al*. (2021), when $\theta = \eta = 0$ and $m = B = 1$, measurement errors are not taken into consideration in the computation of the in-control CV $\left(\gamma_0^*\right)$ and out-of-control CV $\left(\gamma_+^*\right)$, defined in Eqs. (6) and (8), respectively. Thus, when $\theta = \eta = 0$ and $m = B = 1$, the DS CV - ME chart reduces to the basic DS CV chart.

Table 1 also illustrates the effect of m ($\in \{1, 3, 5, 7\}$) on the performance of the DS CV - ME chart, for $\theta = 0.05$, $\eta = 0.28$, $B = 1$, $\gamma_0 = 0.05$ and $n_0 = 5$. It is noticeable that ANOS(δ), for $\delta > 1$, minimally decreases or remains constant as m increases. This indicates that taking multiple measurements does not enormously decrease the negative effect of measurement errors on the DS CV - ME chart. For example, ANOS(1.01) $\in$ {1518.86, 1518.60, 1518.50, 1518.20} for $m \in \{1, 3, 5, 7\}$ (see Table 1). Additionally, it is observed that increasing the slope B improves the sensitivity of the DS CV - ME chart, as a larger B results in a smaller ANOS(δ) ($\delta > 1$) value. As an example, when $\theta = 0.05$, $\eta = 0.28$, $m = 1$, $\gamma_0 = 0.05$ and $n_0 = 5$, ANOS(1.01) $\in$ {1518.86, 1511,.40, 1508.80, 1507.50} for $B \in \{1, 2, 3, 4\}$ (see Table 1).

Table 1: Optimal parameters $n_1, n_2, ku_1^E, kl_1^E, wu^E, wl^E, ku_2^E, kl_2^E$ and the corresponding ANOS(δ) values (boldfaced and italicized) of the DS CV - ME chart with a constant error variance, for $\gamma_0 = 0.05$ and $n_0 = 5$

δ	$\eta = 0.28$ and $m = B = 1$			
	$\theta = 0$	$\theta = 0.01$	$\theta = 0.03$	$\theta = 0.05$
1.01	3, 27, 5, 1.9070, 1.5655, 1.9069, 2.4513, 1.9068 ***(1504.10)***	3, 27, 5, 1.9070, 1.5655, 1.9069, 2.4511, 1.9068 ***(1506.90)***	3, 27, 5, 1.9070, 1.5655, 1.9069, 2.4510, 1.9068 ***(1513.10)***	3, 27, 5, 1.9070, 1.5655, 1.9069, 2.4508, 1.9068) ***(1518.86)***
1.05	3, 27, 5, 1.9070, 1.5655, 1.9069, 2.4513, 1.9068 ***(712.79)***	3, 27, 5, 1.9070, 1.5655, 1.9069, 2.4511, 1.9068 ***(718.96)***	3, 27, 5, 1.9070, 1.5655, 1.9069, 2.4510, 1.9068 ***(731.49)***	3, 27, 5, 1.9070, 1.5655, 1.9069, 2.4508, 1.9068) ***(743.65)***
1.2	3, 27, 4.9892, 1.9070, 1.5655, 1.9069, 2.4514, 1.9068 ***(121.62)***	3, 27, 4.9892, 1.9070, 1.5655, 1.9069, 2.4512, 1.9068 ***(123.87)***	3, 27, 4.9892, 1.9070, 1.5655, 1.9069, 2.4510, 1.9068 ***(128.41)***	3, 27, 4.9892, 1.9070, 1.5655, 1.9069, 2.4508, 1.9068 ***(133.01)***
1.3	3, 25, 4.224, 1.9070, 1.5122, 1.9069, 2.5116, 1.9068 ***(66.92)***	3, 25, 4.4420, 1.9070, 1.5123, 1.9069, 2.5100, 1.9068 ***(68.14)***	3, 25, 4.4805, 1.9070, 1.5125, 1.9069, 2.5071, 1.9068 ***(70.63)***	3, 25, 4.5178, 1.9070, 1.5126, 1.9069, 2.5046, 1.9068 ***(73.17)***
1.4	3, 23, 4.0461, 1.9070, 1.4526, 1.9067, 2.6050, 1.9068 ***(45.47)***	3, 23, 4.0654, 1.9070, 1.4528, 1.9067, 2.6005, 1.9068 ***(46.25)***	3, 23, 4.1038, 1.9070 1.4532, 1.9069, 2.5923, 1.9068 ***(47.85)***	3, 23, 4.1417, 1.9070, 1.4535, 1.9069, 2.5851, 1.9068 ***(49.49)***
2	3, 23, 3.7845, 1.9070, 1.4490, 1.9069, 2.7, 1.9068 ***(21.20)***	3, 23, 3.7840, 1.9070, 1.4490, 1.9069, 2.7, 1.9068 ***(21.45)***	3, 23, 3.7829, 1.9070, 1.4490, 1.9069, 2.7, 1.9068 ***(21.95)***	3, 23, 3.7819, 1.9070, 1.4490, 1.9069, 2.7, 1.9068 ***(22.43)***

Table 1 (Continued)

δ	$\theta = 0$ and $m = B = 1$			
	$\eta = 0$	$\eta = 0.1$	$\eta = 0.3$	$\eta = 0.5$
1.01	3, 27, 5, 1.9070, 1.5655, 1.9069, 2.4508, 1.9068 ***(1503.71)***	3, 27, 5, 1.9070, 1.5655, 1.9069, 2.4510, 1.9068 ***(1504.00)***	3, 27, 5, 1.9070, 1.5655, 1.9069, 2.4514, 1.9068 ***(1504.20)***	3, 27, 5, 1.9070, 1.5655, 1.9069, 2.4523, 1.9068 ***(1504.21)***
1.05	3, 27, 5, 1.9070, 1.5655, 1.9069, 2.4508, 1.9068 ***(712.57)***	3, 27, 5, 1.9070, 1.5655, 1.9069, 2.4510, 1.9068 ***(712.77)***	3, 27, 5, 1.9070, 1.5655, 1.9069, 2.4514, 1.9068 ***(712.85)***	3, 27, 5, 1.9070, 1.5655, 1.9069, 2.4523, 1.9068 ***(713.09)***
1.2	3, 27, 4.9868, 1.9070, 1.5655, 1.9069, 2.4510, 1.9068 ***(121.58)***	3, 27, 4.9871, 1.9070, 1.5655, 1.9069, 2.4511, 1.9068 ***(121.59)***	3, 27, 4.9877, 1.9070, 1.5655, 1.9069, 2.4515, 1.9068 ***(121.63)***	3, 27, 4.9970, 1.9060, 1.5655, 1.9050, 2.4523, 1.9048 ***(121.71)***
1.3	3, 25, 4.42, 1.9070, 1.5122, 1.9069, 2.5112, 1.9068 ***(66.90)***	3, 25, 4.4203, 1.9070, 1.5122, 1.9069, 2.5113, 1.9068 ***(66.90)***	3, 25, 4.4227, 1.9070, 1.5122, 1.9069, 2.5116, 1.9068 ***(66.92)***	3, 25, 4.4280, 1.9060, 1.5122, 1.9050, 2.5124, 1.9048 ***(66.96)***
1.4	3, 23, 4.0441, 1.9070, 1.4526, 1.9067, 2.6048, 1.9068 ***(45.45)***	3, 23, 4.0443, 1.9070, 1.4526, 1.9069, 2.6048, 1.9068 ***(45.46)***	3, 23, 4.0464, 1.9070, 1.4526, 1.9069, 2.6051, 1.9068 ***(45.47)***	3, 23, 4.0507, 1.9060, 1.4526, 1.9050, 2.6058, 1.9048 ***(45.50)***
2	3, 23, 3.7825, 1.9070, 1.4490, 1.9069, 2.7, 1.9068 ***(21.20)***	3, 23, 3.7827, 1.9070, 1.4490, 1.9069, 2.7, 1.9068 ***(21.20)***	3, 23, 3.7848, 1.9070, 1.4490, 1.9069, 2.7, 1.9068 ***(21.20)***	3, 23, 3.7891, 1.9070, 1.4490, 1.9069, 2.7, 1.9068 ***(21.21)***
δ	$\theta = 0.05$, $\eta = 0.28$ and $B = 1$			
	$m = 1$	$m = 3$	$m = 5$	$m = 7$
1.01	3, 27, 5, 1.9070, 1.5655, 1.9069, 2.4508, 1.9068 ***(1518.86)***	3, 27, 5, 1.9070, 1.5655, 1.9069, 2.4505, 1.9068 ***(1518.60)***	3, 27, 5, 1.9070, 1.5655, 1.9069, 2.4504, 1.9068 ***(1518.50)***	3, 27, 5, 1.9070, 1.5655, 1.9069, 2.4503, 1.9068 ***(1518.20)***
1.05	3, 27, 5, 1.9070, 1.5655, 1.9069, 2.4508, 1.9068 ***(743.65)***	3, 27, 5, 1.9070, 1.5655, 1.9069, 2.4505, 1.9068 ***(743.52)***	3, 27, 5, 1.9070, 1.5655, 1.9069, 2.4504, 1.9068 ***(743.44)***	3, 27, 5, 1.9070, 1.5655, 1.9069, 2.4503, 1.9068 ***(743.34)***
1.2	3, 27, 5, 1.9070, 1.5655, 1.9069, 2.4508, 1.9068 ***(133.01)***	3, 27, 5, 1.9070, 1.5655, 1.9069, 2.4505, 1.9068 ***(132.98)***	3, 27, 5, 1.9070, 1.5655, 1.9069, 2.4504, 1.9068 ***(132.97)***	3, 27, 5, 1.9070, 1.5655, 1.9069, 2.4503, 1.9068 ***(132.96)***
1.3	3, 25, 4.5178, 1.9070, 1.5126, 1.9069, 2.5046, 1.9068 ***(73.17)***	3, 26, 4.4899, 1.9070, 1.5390, 1.9069, 2.4861, 1.9068 ***(73.10)***	3, 26, 4.4896, 1.9070, 1.5390, 1.9069, 2.4861, 1.9068 ***(73.10)***	3, 26, 4.4895, 1.9070, 1.5390, 1.9069, 2.4860, 1.9068 ***(73.10)***
1.4	3, 23, 4.1417, 1.9070, 1.4535, 1.9069, 2.5851, 1.9068 ***(49.49)***	3, 23, 4.1405, 1.9070, 1.4535, 1.9069, 2.5849, 1.9068 ***(49.48)***	3, 23, 4.1402, 1.9070, 1.4535, 1.9069, 2.5848, 1.9068 ***(49.48)***	3, 23, 4.1401, 1.9070, 1.4535, 1.9069, 2.5848, 1.9068 ***(49.48)***
2	3, 23, 3.7819, 1.9070, 1.4490, 1.9069, 2.7, 1.9068 ***(22.43)***	3, 23, 3.7807, 1.9070, 1.4490, 1.9069, 2.7, 1.9068 ***(22.43)***	3, 23, 3.7804, 1.9070, 1.4490, 1.9069, 2.7, 1.9068 ***(22.43)***	3, 23, 3.7803, 1.9070, 1.4490, 1.9069, 2.7, 1.9068 ***(22.42)***
δ	$\theta = 0.05$, $\eta = 0.28$ and $m = 1$			
	$B = 1$	$B = 2$	$B = 3$	$B = 4$
1.01	3, 27, 5, 1.9070, 1.5655, 1.9069, 2.4508, 1.9068 ***(1518.86)***	3, 27, 5, 1.9070, 1.5655, 1.9069, 2.4507, 1.9068 ***(1511.40)***	3, 27, 5, 1.9070, 1.5655, 1.9069, 2.4507, 1.9068 ***(1508.80)***	3, 27, 5, 1.9070, 1.5655, 1.9069, 2.4507, 1.9068 ***(1507.50)***

Table 1 (Continued)

1.05	3, 27, 5, 1.9070, 1.5655, 1.9069, 2.4508, 1.9068 ***(743.65)***	3, 27, 5, 1.9070, 1.5655, 1.9069, 2.4507, 1.9068 ***(728.27)***	3, 27, 5, 1.9070, 1.5655, 1.9069, 2.4507, 1.9068 ***(723.06)***	3, 27, 5, 1.9070, 1.5655, 1.9069, 2.4507, 1.9068 ***(720.43)***
1.2	3, 27, 5, 1.9070, 1.5655, 1.9069, 2.4508, 1.9068 ***(133.01)***	3, 27, 5, 1.9070, 1.5655, 1.9069, 2.4507, 1.9068 ***(127.23)***	3, 27, 5, 1.9070, 1.5655, 1.9069, 2.4508, 1.9068 ***(125.34)***	3, 27, 5, 1.9070, 1.5655, 1.9069, 2.4508, 1.9068 ***(124.40)***
1.3	3, 25, 4.5178, 1.9070, 1.5126, 1.9069, 2.5046, 1.9068 ***(73.17)***	3, 25, 4.4692, 1.9070, 1.5124, 1.9069, 2.5076, 1.9068 ***(69.99)***	3, 25, 4.4529, 1.9070, 1.5124, 1.9069, 2.5087, 1.9068 ***(68.95)***	3, 25, 4.4447, 1.9070, 1.5123, 1.9069, 2.5093, 1.9068 ***(68.43)***
1.4	3, 23, 4.1417, 1.9070, 1.4535, 1.9069, 2.5851, 1.9068 ***(49.49)***	3, 23, 4.0928, 1.9070, 1.4531, 1.9069, 2.5940, 1.9068 ***(47.44)***	3, 23, 4.0765, 1.9070, 1.4529, 1.9069, 2.5974, 1.9068 ***(46.77)***	3, 23, 4.0684, 1.9070, 1.4529, 1.9069, 2.5992, 1.9068 ***(46.44)***
2	3, 23, 3.7819, 1.9070, 1.4490, 1.9069, 2.7, 1.9068 ***(22.43)***	3, 23, 3.7817, 1.9070, 1.4490, 1.9069, 2.7, 1.9068 ***(21.82)***	3, 23, 3.7817, 1.9070, 1.4490, 1.9069, 2.7, 1.9068 ***(21.61)***	3, 23, 3.7819, 1.9070, 1.4490, 1.9069, 2.7, 1.9068 ***(21.51)***

Table 2: Optimal parameters $n_1, n_2, ku_1^E, kl_1^E, wu^E, wl^E, ku_2^E, kl_2^E$ and the corresponding $\text{EANOS}(\delta_{\min}, \delta_{\max})$ values (boldfaced and italicized) of the DS CV - ME chart with a constant error variance, for γ_0 = 0.05 and n_0 = 5

($\delta_{\min}$, $\delta_{\max}$)	η = 0.28 and m = B = 1			
	θ = 0	θ = 0.01	θ = 0.03	θ = 0.05
(1.01, 1.05)	3, 27, 5, 1.9070, 1.5655, 1.9069, 2.4513, 1.9068 ***(1047.60)***	3, 27, 5, 1.9070, 1.5655, 1.9060, 2.4511, 1.9068 ***(1052.83)***	3, 27, 5, 1.9070, 1.5655, 1.9060, 2.4509, 1.9068 ***(1063.51)***	3, 27, 5, 1.9070, 1.5655, 1.9060, 2.4508, 1.9068 ***(1074.09)***
(1.2, 1.3)	3, 27, 4.6843, 1.9070, 1.5650, 1.9069, 2.4583, 1.9068 ***(89.31)***	3, 27, 4.7026, 1.9070, 1.5650, 1.9069, 2.4576, 1.9068 ***(90.94)***	3, 27, 4.7381, 1.9070, 1.5651, 1.9069, 2.4563, 1.9068 ***(94.26)***	3, 27, 4.7725, 1.9070, 1.5651, 1.9069, 2.4551, 1.9068 ***(97.63)***
(1.4, 2.0)	3, 23, 3.7845, 1.9070, 1.4490, 1.9069, 2.7, 1.9068 ***(28.45)***	3, 23, 3.7840, 1.9070, 1.4490, 1.9069, 2.7, 1.9068 ***(28.83)***	3, 23, 3.7829, 1.9070, 1.4490, 1.9069, 2.7, 1.9068 ***(29.62)***	3, 23, 3.7819, 1.9070, 1.4490, 1.9069, 2.7, 1.9068 ***(30.42)***
($\delta_{\min}$, $\delta_{\max}$)	θ = 0 and m = B = 1			
	η = 0	η = 0.1	η = 0.3	η = 0.5
(1.01, 1.05)	3, 27, 5, 1.9070, 1.5655, 1.9069, 2.4509, 1.9068 ***(1047.49)***	3, 27, 5, 1.9070, 1.5655, 1.9060, 2.4510, 1.9068 ***(1047.60)***	3, 27, 5, 1.9070, 1.5655, 1.9060, 2.4514, 1.9068 ***(1047.67)***	3, 27, 5, 1.9070, 1.5655, 1.9060, 2.4523, 1.9068 ***(1047.84)***
(1.2, 1.3)	3, 27, 4.6815, 1.9070, 1.5650, 1.9067, 2.4580, 1.9068 ***(89.28)***	3, 27, 4.6819, 1.9070, 1.5650, 1.9068, 2.4580, 1.9068) ***(89.29)***	3, 27, 4.6846, 1.9070, 1.5650, 1.9068, 2.4584, 1.9068) ***(89.31)***	3, 27, 4.6903, 1.9060, 1.5650, 1.9052, 2.4591, 1.9068 ***(89.37)***
(1.4, 2.0)	3, 23, 3.7825, 1.9070, 1.4490, 1.9066, 2.7, 1.9068 ***(28.44)***	3, 23, 3.7827, 1.9070, 1.4490, 1.9066, 2.7, 1.9068 ***(28.44)***	3, 23, 3.7848, 1.9070, 1.4490, 1.9066, 2.7, 1.9068 ***(28.45)***	3, 23, 3.7893, 1.9070, 1.4490, 1.9066, 2.7, 1.9068 ***(28.47)***

Table 2 (Continued)

$(\delta_{\min}, \delta_{\max})$	$\theta = 0.05$, $\eta = 0.28$ and $B = 1$			
	$m = 1$	$m = 3$	$m = 5$	$m = 7$
(1.01, 1.05)	3, 27, 5, 1.9070, 1.5655, 1.9069, 2.4508, 1.9068 ***(1074.09)***	3, 27, 5, 1.9070, 1.5655, 1.9060, 2.4505, 1.9068 ***(1073.92)***	3, 27, 5, 1.9070, 1.5655, 1.9060, 2.4504, 1.9068 ***(1073.80)***	3, 27, 5, 1.9070, 1.5655, 1.9060, 2.4502, 1.9068 ***(1073.44)***
(1.2, 1.3)	3, 27, 4.7725, 1.9070, 1.5651, 1.9069, 2.4551, 1.9068 ***(97.63)***	3, 27, 4.7708, 1.9070, 1.5651, 1.9069, 2.4549, 1.9068 ***(97.61)***	3, 27, 4.7704, 1.9070, 1.5651, 1.9067, 2.4548, 1.9068 ***(97.60)***	3, 27, 4.7703, 1.9070, 1.5651, 1.9069, 2.4548, 1.9068 ***(97.60)***
(1.4, 2.0)	3, 23, 3.7819, 1.9070, 1.4490, 1.9069, 2.7, 1.9068 ***(30.42)***	3, 23, 3.7807, 1.9070, 1.4490, 1.9069, 2.7, 1.9068 ***(30.41)***	3, 23, 3.7804, 1.9070, 1.4490, 1.9069, 2.7, 1.9068 ***(30.41)***	3, 23, 3.7803, 1.9070, 1.4490, 1.9069, 2.7, 1.9068 ***(30.41)***
$(\delta_{\min}, \delta_{\max})$	$\theta = 0.05$, $\eta = 0.28$ and $m = 1$			
	$B = 1$	$B = 2$	$B = 3$	$B = 4$
(1.01, 1.05)	3, 27, 5, 1.9070, 1.5655, 1.9069, 2.4508, 1.9068 ***(1074.09)***	3, 27, 5, 1.9070, 1.5655, 1.9060, 2.4507, 1.9068 ***(1060.88)***	3, 27, 5, 1.9070, 1.5655, 1.9060, 2.4507, 1.9068 ***(1056.37)***	3, 27, 5, 1.9070, 1.5655, 1.9060, 2.4507, 1.9068 ***(1054.09)***
(1.2, 1.3)	3, 27, 4.7725, 1.9070, 1.5651, 1.9069, 2.4551, 1.9068 ***(97.63)***	3, 27, 4.7273, 1.9070, 1.5651, 1.9067, 2.4563, 1.9068 ***(93.40)***	3, 27, 4.7122, 1.9070, 1.5650, 1.9067, 2.4568, 1.9068 ***(92.01)***	3, 27, 4.7045, 1.9070, 1.5650, 1.9067, 2.4571, 1.9068 ***(91.33)***
(1.4, 2.0)	3, 23, 3.7819, 1.9070, 1.4490, 1.9069, 2.7, 1.9068 ***(30.42)***	3, 23, 3.7817 1.9070, 1.4490, 1.9069, 2.7, 1.9068 ***(29.41)***	3, 23, 3.7818 1.9070, 1.4490, 1.9069, 2.7, 1.9068 ***(29.09)***	3, 23, 3.7819 1.9070, 1.4490, 1.9069, 2.7, 1.9068 ***(28.92)***

In monitoring the process CV, there are situations where the exact shift size (δ) is unknown. To address this setback, the DS CV - ME chart can be optimally designed to minimize $\text{EANOS}\left(\delta_{\min}, \delta_{\max}\right)$. This study considers $\left(\delta_{\min}, \delta_{\max}\right) \in$ {(1.01, 1.05), (1.2, 1.3), (1.4, 2.0)}. Table 2 displays the optimal parameters and corresponding $\text{EANOS}\left(\delta_{\min}, \delta_{\max}\right)$ values, based on similar values of θ, η, m, B, γ_0 and n_0 used in minimizing ANOS(δ). Similar to the case of minimizing ANOS(δ) ($\delta > 1$) mentioned above, an increase in θ decreases the out-of-control detection speed of the DS CV - ME chart because it leads to an increase in the $\text{EANOS}\left(\delta_{\min}, \delta_{\max}\right)$ value. For instance, EANOS(1.01, 1.05) $\in$ {1047.60, 1052.83, 1063.51, 1074.09} for $\theta \in$ {0, 0.01, 0.03, 0.05} when $\eta = 0.28$, $m = 1$, $B = 1$, $\gamma_0 = 0.05$ and $n_0 = 5$ (see Table 2). The results in Table 2 show that changes in η and m have negligible effect on $\text{EANOS}\left(\delta_{\min}, \delta_{\max}\right)$. However, increasing the value of B improves the DS CV - ME chart's performance because it results in a decrease in EANOS $\left(\delta_{\min}, \delta_{\max}\right)$. For example, EANOS(1.2, 1.3) $\in$ {97.63, 93.40, 92.01, 91.33} for $B \in$ {1, 2, 3, 4} when $\theta = 0.05$, $\eta = 0.28$, $m = 1$, $\gamma_0 = 0.05$ and $n_0 = 5$ (see Table 2). The numerical results presented here align with the findings in Tran *et al*. (2019a), Nguyen *et al*. (2019), Saha *et al*. (2021) and Lee *et al*. (2020).

7.2. *Performance of the DS CV – ME chart with an error variance which is a linearly increasing function of the mean*

Table 3 summarizes the optimal parameters and corresponding ANOS(δ) values for various combinations of θ, ω, ϕ, m and B when the exact shift size is known and the variance of the error term is a linearly increasing function of the mean. Results are given for $\theta \in \{0, 0.01, 0.03, 0.05\}$ when $\omega = \phi = 0$, $m = B = 1$, $\gamma_0 = 0.05$ and $n_0 = 5$. Following Lee *et al*. (2020) and Saha *et al*. (2021), when $\theta = \omega = \phi = 0$ and $m = B = 1$, the in-control CV $\left(\gamma_0^*\right)$ and out-of-control CV $\left(\gamma_+^*\right)$ in Eqs. (13) and (14), respectively, reduce to the in-control and out-of-control CVs without measurement errors. Thus, when $\theta = \omega = \phi = 0$, $m = B = 1$, the DS CV - ME chart under the error variance which is a linearly increasing function of the mean becomes the basic DS CV chart. In Table 3, it is seen that ANOS(δ) ($\delta > 1$) increases with θ. For example, ANOS(1.3) $\in$ {66.90, 68.12, 70.61, 73.15} for $\theta \in \{0, 0.01, 0.03, 0.05\}$ (see Table 3). This indicates that an increase in θ affects the DS CV - ME chart's performance negatively.

Table 3 also provides the optimal parameters and corresponding ANOS(δ) values for $\omega \in \{0, 0.1, 0.2, 0.3\}$ when $\theta = \phi = 0$, as well as that for $\phi \in \{0, 0.1, 0.2, 0.3\}$ when $\theta = \omega = 0$, where both cases involve $m = B = 1$, $\gamma_0 = 0.05$ and $n_0 = 5$. Table 3 clearly shows that changes in ω does not affect ANOS(δ). It is noticed in Table 3 that ANOS(δ) increases with ϕ. For example, when $\theta = \omega = 0$, $m = B = 1$, $\gamma_0 = 0.05$ and $n_0 = 5$, ANOS(1.05) $\in$ {712.57, 715.64, 724.48, 738.26} for $\phi \in \{0, 0.1, 0.2, 0.3\}$ (see Table 3). This shows that the ANOS(δ) performance of the DS CV - ME chart worsens as ϕ increases. Moreover, the effect of m and B on the DS CV - ME chart under the error variance which is a linearly increasing function of the mean is analyzed. Values of $m \in \{1, 3, 5, 7\}$ for $\theta = 0.05$, $\omega = \phi = 0.1$ and $B = 1$, as well as $B \in \{1, 2, 3, 4\}$ for $\theta = 0.05$, $\omega = \phi = 0.1$ and $m = 1$ are considered. It is seen in Table 3 that increasing m or taking multiple measurements per item does not lead to an improved ANOS(δ) performance.

Table 3: Optimal parameters $n_1, n_2, ku_1^E, kl_1^E, wu^E, wl^E, ku_2^E, kl_2^E$ and the corresponding ANOS(δ) values (boldfaced and italicized) of the DS CV- ME chart with an error variance which is a linearly increasing function of the mean, for $\gamma_0 = 0.05$ and $n_0 = 5$

δ	$\omega = \phi = 0$ and $m = B = 1$			
	$\theta = 0$	$\theta = 0.01$	$\theta = 0.03$	$\theta = 0.05$
1.01	3, 27, 5, 1.9070, 1.5655, 1.9069, 2.4508, 1.9068 ***(1503.71)***	3, 27, 5, 1.9070, 1.5655, 1.9069, 2.4508, 1.9068 ***(1507.10)***	3, 27, 5, 1.9070, 1.5655, 1.9069, 2.4506, 1.9068 ***(1513.00)***	3, 27, 5, 1.9070, 1.5655, 1.9069, 2.4504, 1.9068 ***(1518.70)***
1.05	3, 27, 5, 1.9070, 1.5655, 1.9069, 2.4508, 1.9068 ***(712.57)***	3, 27, 5, 1.9070, 1.5655, 1.9069, 2.4508, 1.9068 ***(718.98)***	3, 27, 5, 1.9070, 1.5655, 1.9069, 2.4506, 1.9068 ***(731.37)***	3, 27, 5, 1.9070, 1.5655, 1.9069, 2.4504, 1.9068 ***(743.52)***
1.2	3, 27, 4.9868, 1.9070, 1.5655, 1.9069, 2.4510, 1.9068 ***(121.58)***	3, 27, 4.9985, 1.9070, 1.5655, 1.9069, 2.4508, 1.9068 ***(123.83)***	3, 27, 4.9991, 1.9070, 1.5655, 1.9068, 2.4506, 1.9068 ***(128.37)***	3, 27, 5, 1.9070, 1.5655, 1.9069, 2.4504, 1.9068 ***(132.97)***
1.3	3, 25, 4.42, 1.9070, 1.5122, 1.9069, 2.5112, 1.9068 ***(66.90)***	3, 25, 4.4396, 1.9070, 1.5123, 1.9069, 2.5097, 1.9068 ***(68.12)***	3, 25, 4.4782, 1.9070, 1.5125, 1.9069, 2.5068, 1.9068 ***(70.61)***	3, 25, 4.5155, 1.9070, 1.5126, 1.9069, 2.5043, 1.9068 ***(73.15)***

Table 3 (Continued)				
1.4	3, 23, 4.0441, 1.9070, 1.4526, 1.9067, 2.6048, 1.9068 ***(45.45)***	3, 23, 4.0634, 1.9070, 1.4528, 1.9067, 2.6048, 1.9068 ***(46.24)***	3, 23, 4.1019, 1.9070, 1.4532, 1.9068, 2.5920, 1.9068 ***(47.84)***	3, 23, 4.1399, 1.9070, 1.4535, 1.9068, 2.5848, 1.9068 ***(49.48)***
2	3, 23, 3.7825, 1.9070, 1.4490, 1.9069, 2.7, 1.9068 ***(21.20)***	3, 23, 3.7819, 1.9070, 1.4490, 1.9069, 2.7, 1.9068 ***(21.45)***	3, 23, 3.7810, 1.9070, 1.4490, 1.9069, 2.7, 1.9068 ***(21.94)***	3, 23, 3.7800, 1.9070, 1.4490, 1.9069, 2.7, 1.9068 ***(22.43)***
δ	$\theta = \phi = 0$ and $m = B = 1$			
	$\omega = 0$	$\omega = 0.1$	$\omega = 0.2$	$\omega = 0.3$
1.01	3, 27, 5, 1.9070, 1.5655, 1.9069, 2.4508, 1.9068 ***(1503.71)***	3, 27, 5, 1.9070, 1.5655, 1.9069, 2.4509, 1.9068 ***(1503.86)***	3, 27, 5, 1.9070, 1.5655, 1.9069, 2.4511, 1.9068 ***(1504.00)***	3, 27, 5, 1.9070, 1.5655, 1.9069, 2.4514, 1.9068 ***(1504.20)***
1.05	3, 27, 5, 1.9070, 1.5655, 1.9069, 2.4508, 1.9068 ***(712.57)***	3, 27, 5, 1.9070, 1.5655, 1.9069, 2.4509, 1.9068 ***(712.65)***	3, 27, 5, 1.9070, 1.5655, 1.9069, 2.4511, 1.9068 ***(712.74)***	3, 27, 5, 1.9070, 1.5655, 1.9069, 2.4514, 1.9068 ***(712.85)***
1.2	3, 27, 4.9868, 1.9070, 1.5655, 1.9069, 2.4510, 1.9068 ***(121.58)***	3, 27, 4.9868, 1.9070, 1.5655, 1.9069, 2.4511, 1.9068 ***(121.59)***	3, 27, 4.9883, 1.9070, 1.5655, 1.9069, 2.4512, 1.9068 ***(121.60)***	3, 27, 4.9904, 1.9070, 1.5655, 1.9069, 2.4514, 1.9068 ***(121.62)***
1.3	3, 25, 4.42, 1.9070, 1.5122, 1.9069, 2.5112, 1.9068 ***(66.90)***	3, 25, 4.4203, 1.9070, 1.5122, 1.9069, 2.5113, 1.9068 ***(66.90)***	3, 25, 4.4212, 1.9070, 1.5122, 1.9069, 2.5114, 1.9068 ***(66.91)***	3, 25, 4.4227, 1.9070, 1.5122, 1.9069, 2.5116, 1.9068 ***(66.92)***
1.4	3, 23, 4.0441, 1.9070, 1.4526, 1.9067, 2.6048, 1.9068 ***(45.45)***	3, 23, 4.0443, 1.9070, 1.4526, 1.9069, 2.6048, 1.9068 ***(45.46)***	2, 23, 4.0451, 1.9070, 1.4526, 1.9069, 2.6049, 1.9068 ***(45.46)***	3, 23, 4.0464, 1.9070, 1.4526, 1.9069, 2.6051, 1.9068 ***(45.47)***
2	3, 23, 3.7825, 1.9070, 1.4490, 1.9069, 2.7, 1.9068 ***(21.20)***	3, 23, 3.7827, 1.9070, 1.4490, 1.9069, 2.7, 1.9068 ***(21.20)***	3, 23, 3.7835, 1.9070, 1.4490, 1.9069, 2.7, 1.9068 ***(21.20)***	3, 23, 3.7848, 1.9070, 1.4490, 1.9069, 2.7, 1.9068 ***(21.20)***
δ	$\theta = \omega = 0$ and $m = B = 1$			
	$\phi = 0$	$\phi = 0.1$	$\phi = 0.2$	$\phi = 0.3$
1.01	3, 27, 5, 1.9070, 1.5655, 1.9069, 2.4508, 1.9068 ***(1503.71)***	3, 27, 5, 1.9070, 1.5655, 1.9069, 2.4509, 1.9068 ***(1505.38)***	3, 27, 5, 1.9070, 1.5655, 1.9069, 2.4511, 1.9068 ***(1509.95)***	3, 27, 5, 1.9070, 1.5655, 1.9069, 2.4513, 1.9068 ***(1516.64)***
1.05	3, 27, 5, 1.9070, 1.5655, 1.9069, 2.4508, 1.9068 ***(712.57)***	3, 27, 5, 1.9070, 1.5655, 1.9069, 2.4509, 1.9068 ***(715.64)***	3, 27, 5, 1.9070, 1.5655, 1.9069, 2.4511, 1.9068 ***(724.48)***	3, 27, 5, 1.9070, 1.5655, 1.9069, 2.4513, 1.9068 ***(738.26)***
1.2	3, 27, 4.9868, 1.9070, 1.5655, 1.9069, 2.4510, 1.9068 ***(121.58)***	3, 27, 4.9931, 1.9070, 1.5655, 1.9069, 2.4510, 1.9068 ***(122.52)***	3, 27, 4.9982, 1.9070, 1.5655, 1.9069, 2.4511, 1.9068 ***(125.30)***	3, 27, 4.9999, 1.9070, 1.5655, 1.9069, 2.4513, 1.9068 ***(129.82)***
1.3	3, 25, 4.42, 1.9070, 1.5122, 1.9069, 2.5112, 1.9068 ***(66.90)***	3, 25, 4.4281, 1.9070, 1.5122, 1.9069, 2.5107, 1.9068 ***(67.37)***	3, 25, 4.4518, 1.9070, 1.5123, 1.9069, 2.5092, 1.9068 ***(68.77)***	3, 25, 4.4893, 1.9070, 1.5125, 1.9069, 2.5070, 1.9068 ***(71.06)***
1.4	3, 23, 4.0441, 1.9070, 1.4526, 1.9067, 2.6048, 1.9068 ***(45.45)***	3, 23, 4.0514, 1.9070, 1.4527, 1.9067, 2.6032, 1.9068 ***(45.74)***	3, 23, 4.0730, 1.9070, 1.4529, 1.9067, 2.5987, 1.9069 ***(46.57)***	3, 23, 4.1076, 1.9070, 1.4532, 1.9069, 2.5922, 1.9068 ***(47.94)***

Table 3 (Continued)				
2	3, 23, 3.7825, 1.9070, 1.4490, 1.9069, 2.7, 1.9068 ***(21.20)***	3, 23, 3.7827, 1.9070, 1.4490, 1.9069, 2.7, 1.9068 ***(21.26)***	3, 23, 3.7835, 1.9070, 1.4490, 1.9069, 2.7, 1.9068 ***(21.45)***	3, 23, 3.7848, 1.9070, 1.4490, 1.9069, 2.7, 1.9068 ***(21.75)***
δ	θ = 0.05, B = 1 and ω = ϕ = 0.1			
	m = 1	m = 3	m = 5	m = 7
1.01	3, 27, 4.9999, 1.9070, 1.5655, 1.9068, 2.4505, 1.9067 ***(1520.23)***	3, 27, 5, 1.9070, 1.5655, 1.9069, 2.4505, 1.9068 ***(1519.40)***	3, 27, 5, 1.9070, 1.5655, 1.9069, 2.4504, 1.9068 ***(1518.90)***	3, 27, 5, 1.9070, 1.5655, 1.9069, 2.4504, 1.9068 ***(1518.85)***
1.05	3, 27, 4.9999, 1.9070, 1.5655, 1.9068, 2.4505, 1.9067 ***(746.68)***	3, 27, 5, 1.9070, 1.5655, 1.9069, 2.4505, 1.9068 ***(744.67)***	3, 27, 5, 1.9070, 1.5655, 1.9069, 2.4504, 1.9068 ***(744.13)***	3, 27, 5, 1.9070, 1.5655, 1.9069, 2.4504, 1.9068 ***(743.96)***
1.2	3, 27, 4.9996, 1.9070, 1.5655, 1.9068, 2.4505, 1.9068 ***(134.04)***	3, 27, 5, 1.9070, 1.5655, 1.9068, 2.4505, 1.9068 ***(133.34)***	3, 27, 4.9996, 1.9070, 1.5655, 1.9068, 2.4504, 1.9068 ***(133.18)***	3, 27, 5, 1.9070, 1.5655, 1.9068, 2.4504, 1.9068 ***(133.12)***
1.3	3, 25, 4.5244, 1.9070, 1.5126, 1.9069, 2.5042, 1.9068 ***(73.71)***	3, 25, 4.5184, 1.9070, 1.5126, 1.9069, 2.5042, 1.9068 ***(73.34)***	3, 25, 4.5173, 1.9070, 1.5126, 1.9069, 2.5042, 1.9068 ***(73.26)***	3, 25, 4.5127, 1.9070, 1.5126, 1.9069, 2.5042, 1.9068 ***(73.23)***
1.4	3, 23, 4.1480, 1.9070, 1.4536, 1.9069, 2.5836, 1.9068 ***(49.82)***	3, 23, 4.1426, 1.9070, 1.4535, 1.9069, 2.5844, 1.9068 ***(49.59)***	3, 23, 4.1415, 1.9070, 1.4535, 1.9069, 2.5845, 1.9068 ***(49.55)***	3, 23, 4.1410, 1.9070, 1.4535, 1.9069, 2.5846, 1.9068 ***(49.53)***
2	3, 23, 3.7805, 1.9070, 1.4490, 1.9069, 2.7, 1.9068 ***(22.50)***	3, 23, 3.7802, 1.9070, 1.4490, 1.9069, 2.7, 1.9068 ***(22.45)***	3, 23, 3.7802, 1.9070, 1.4490, 1.9069, 2.7, 1.9068 ***(22.44)***	3, 23, 3.7801, 1.9070, 1.4490, 1.9069, 2.7, 1.9068 ***(22.44)***
δ	θ = 0.05, m = 1 and ω = ϕ = 0.1			
	B = 1	B = 2	B = 3	B = 4
1.01	3, 27, 4.9999, 1.9070, 1.5655, 1.9068, 2.4505, 1.9067 ***(1520.23)***	3, 27, 5, 1.9070, 1.5655, 1.9069, 2.4507, 1.9068 ***(1511.99)***	3, 27, 5, 1.9070, 1.5655, 1.9069, 2.4507, 1.9068 ***(1509.10)***	3, 27, 5, 1.9070, 1.5655, 1.9069, 2.4508, 1.9068 ***(1507.97)***
1.05	3, 27, 4.9999, 1.9070, 1.5655, 1.9068, 2.4505, 1.9067 ***(746.68)***	3, 27, 5, 1.9070, 1.5655, 1.9069, 2.4507, 1.9068 ***(729.11)***	3, 27, 5, 1.9070, 1.5655, 1.9069, 2.4507, 1.9068 ***(723.43)***	3, 27, 5, 1.9070, 1.5655, 1.9069, 2.4508, 1.9068 ***(720.76)***
1.2	3, 27, 4.9996, 1.9070, 1.5655, 1.9068, 2.4505, 1.9068 ***(134.04)***	3, 27, 4.9989, 1.9070, 1.5655, 1.9068, 2.4507, 1.9068 ***(127.48)***	3, 27, 4.9995, 1.9070, 1.5655, 1.9069, 2.4507, 1.9068 ***(125.44)***	3, 27, 4.9998, 1.9070, 1.5655, 1.9069, 2.4508, 1.9068 ***(124.46)***
1.3	3, 25, 4.5244, 1.9070, 1.5126, 1.9069, 2.5042, 1.9068 ***(73.71)***	3, 25, 4.4708, 1.9070, 1.5124, 1.9069, 2.5042, 1.9068 ***(70.11)***	3, 25, 4.4536, 1.9070, 1.5124, 1.9069, 2.5074, 1.9068 ***(69.00)***	3, 24, 4.4451, 1.9070, 1.5123, 1.9069, 2.5092, 1.9068 ***(68.46)***
1.4	3, 23, 4.1480, 1.9070, 1.4536, 1.9069, 2.5836, 1.9068 ***(49.82)***	3, 23, 4.0943, 1.9070, 1.4531, 1.9069, 2.5936, 1.9068 ***(47.51)***	3, 23, 4.0772, 1.9070, 1.4529, 1.9069, 2.5972, 1.9068 ***(46.80)***	3, 23, 4.0688, 1.9070, 1.4529, 1.9069, 2.5990, 1.9068 ***(46.45)***
2	3, 23, 3.7805, 1.9070, 1.4490, 1.9069, 2.7, 1.9068 ***(22.50)***	3, 23, 3.7813, 1.9070, 1.4490, 1.9069, 2.7, 1.9068 ***(21.83)***	3, 23, 3.7817, 1.9070, 1.4490, 1.9069, 2.7, 1.9068 ***(21.62)***	3, 23, 3.7819, 1.9070, 1.4490, 1.9069, 2.7, 1.9068 ***(21.51)***

However, Table 3 shows that as the value of B becomes larger, the ANOS(δ) (δ > 1) decreases, which translates into an improved DS CV - ME chart's performance. For example, for δ = 1.05, ANOS(δ) $\in$ {746.68, 729.11, 723.43, 720.76} for B $\in$ {1, 2, 3, 4} when θ = 0.05, $\omega = \phi$ = 0.1, m = 1, γ_0 = 0.05 and n_0 = 5 (see Table 3).

Table 4: Optimal parameters $n_1, n_2, ku_1^E, kl_1^E, wu^E, wl^E, ku_2^E, kl_2^E$ and the corresponding EANOS $(\delta_{min}, \delta_{max})$ values (boldfaced and italicized) of the DS CV - ME chart with an error variance which is a linearly increasing function of the mean, for γ_0 = 0.05 and n_0 = 5

(δ_{min}, δ_{max})	$\omega = \phi$ = 0 and $m = B$ = 1			
	θ = 0	θ = 0.01	θ = 0.03	θ = 0.05
(1.01, 1.05)	3, 27, 5, 1.9070, 1.5655, 1.9069, 2.4508, 1.9068 ***(1047.30)***	3, 27, 5, 1.9070, 1.5655, 1.9069, 2.4508, 1.9068 ***(1052.93)***	3, 27, 5, 1.9070, 1.5655, 1.9069, 2.4506, 1.9068 ***(1063.58)***	3, 27, 5, 1.9070, 1.5655, 1.9069, 2.4504, 1.9068 ***(1073.93)***
(1.2, 1.3)	3, 27, 4.6815, 1.9070, 1.5650, 1.9067, 2.4580, 1.9068 ***(89.28)***	3, 27, 4.6998, 1.9070, 1.5650, 1.9069, 2.4573, 1.9068 ***(90.92)***	3, 27, 4.7355, 1.9070, 1.5651, 1.9067, 2.4559, 1.9068 ***(94.23)***	3, 27, 4.7699, 1.9070, 1.5651, 1.9067, 2.4548, 1.9068 ***(97.60)***
(1.4, 2.0)	3, 23, 3.7825, 1.9070, 1.4490, 1.9066, 2.7, 1.9068 ***(28.44)***	3, 23, 3.7819, 1.9070, 1.4490, 1.9069, 2.7, 1.9068 ***(28.83)***	3, 23, 3.7810, 1.9070, 1.4490, 1.9069, 2.7, 1.9068 ***(29.61)***	3, 23, 3.7800, 1.9070, 1.4490, 1.9069, 2.7, 1.9068 ***(30.41)***
(δ_{min}, δ_{max})	$\theta = \phi$ = 0 and $m = B$ = 1			
	ω = 0	ω = 0.1	ω = 0.2	ω = 0.3
(1.01, 1.05)	3, 27, 5, 1.9070, 1.5655, 1.9069, 2.4508, 1.9068 ***(1047.30)***	3, 27, 5, 1.9070, 1.5655, 1.9069, 2.4509, 1.9068 ***(1047.40)***	3, 27, 5, 1.9070, 1.5655, 1.9069, 2.4509, 1.9068 ***(1047.53)***	3, 27, 5, 1.9070, 1.5655, 1.9069, 2.4514, 1.9068 ***(1047.67)***
(1.2, 1.3)	3, 27, 4.6815, 1.9070, 1.5650, 1.9067, 2.4580, 1.9068 ***(89.28)***	3, 27, 4.6819, 1.9070, 1.5650, 1.9067, 2.4580, 1.9068) ***(89.29)***	3, 27, 4.6829, 1.9070, 1.5650, 1.9066, 2.4582, 1.9068) ***(89.31)***	3, 27, 4.6847, 1.9070, 1.5650, 1.9069, 2.4584, 1.9068 ***(89.32)***
(1.4, 2.0)	3, 23, 3.7825, 1.9070, 1.4490, 1.9066, 2.7, 1.9068 ***(28.44)***	3, 23, 3.7827, 1.9070, 1.4490, 1.9069, 2.7, 1.9068 ***(28.44)***	3, 23, 3.7835, 1.9070, 1.4490, 1.9069, 2.7, 1.9068 ***(28.45)***	3, 23, 3.7848, 1.9070, 1.4490, 1.9069, 2.7, 1.9068 ***(28.46)***
(δ_{min}, δ_{max})	$\theta = \omega$ = 0 and $m = B$ = 1			
	ϕ = 0	ϕ = 0.1	ϕ = 0.2	ϕ = 0.3
(1.01, 1.05)	3, 27, 5, 1.9070, 1.5655, 1.9069, 2.4508, 1.9068 ***(1047.30)***	3, 27, 5, 1.9070, 1.5655, 1.9069, 2.4509, 1.9068 ***(1050.34)***	3, 27, 5, 1.9070, 1.5655, 1.9069, 2.4511, 1.9068 ***(1059.01)***	3, 27, 5, 1.9070, 1.5655, 1.9069, 2.4513, 1.9068 ***(1072.44)***
(1.2, 1.3)	3, 27, 4.6815, 1.9070, 1.5650, 1.9067, 2.4580, 1.9068 ***(89.28)***	3, 27, 4.6895, 1.9070, 1.5650, 1.9069, 2.4578, 1.9068 ***(90.12)***	3, 27, 4.7128, 1.9070, 1.5650, 1.9069, 2.4572, 1.9068 ***(92.60)***	3, 27, 4.7493, 1.9070, 1.5651, 1.9066, 2.4563, 1.9068 ***(96.67)***
(1.4, 2.0)	3, 23, 3.7825, 1.9070, 1.4490, 1.9066, 2.7, 1.9068 ***(28.44)***	3, 23, 3.7827, 1.9070, 1.4490, 1.9069, 2.7, 1.9068 ***(28.60)***	3, 23, 3.7835, 1.9070, 1.4490, 1.9069, 2.7, 1.9068 ***(29.07)***	3, 23, 3.7848, 1.9070, 1.4490, 1.9069, 2.7, 1.9068 ***(29.83)***

Table 4 (Continued)

$(\delta_{\min}, \delta_{\max})$	θ = 0.05, B = 1 and $\omega = \phi$ = 0.1			
	m = 1	m = 3	m = 5	m = 7
(1.01, 1.05)	3, 27, 4.9999, 1.9070, 1.5655, 1.9068, 2.4505, 1.9067 ***(1077.00)***	3, 27, 5, 1.9070, 1.5655, 1.9069, 2.4505, 1.9068 ***(1075.09)***	3, 27, 5, 1.9070, 1.5655, 1.9069, 2.4504, 1.9068 ***(1074.51)***	3, 27, 5, 1.9070, 1.5655, 1.9069, 2.4504, 1.9068 ***(1074.34)***
(1.2, 1.3)	3, 27, 4.7781, 1.9070, 1.5652, 1.9067, 2.4547, 1.9068 ***(98.56)***	3, 27, 4.7727, 1.9070, 1.5651, 1.9067, 2.4547, 1.9068 ***(97.92)***	3, 27, 4.7716, 1.9070, 1.5651, 1.9067, 2.4547, 1.9068 ***(97.80)***	3, 27, 4.7711, 1.9070, 1.5651, 1.9067, 2.4548, 1.9068 ***(97.74)***
(1.4, 2.0)	3, 23, 3.7805, 1.9070, 1.4490, 1.9069, 2.7, 1.9068 ***(30.60)***	3, 23, 3.7802, 1.9070, 1.4490, 1.9069, 2.7, 1.9068 ***(30.47)***	3, 23, 3.7801 1.9070, 1.4490, 1.9069, 2.7, 1.9068 ***(30.45)***	3, 23, 3.7800 1.9070, 1.4490, 1.9069, 2.7, 1.9068 ***(30.44)***
$(\delta_{\min}, \delta_{\max})$	θ = 0.05, m = 1 and $\omega = \phi$ = 0.1			
	B =1	B = 2	B = 3	B = 4
(1.01, 1.05)	3, 27, 4.9999, 1.9070, 1.5655, 1.9068, 2.4505, 1.9067 ***(1077.00)***	3, 27, 5, 1.9070, 1.5655, 1.9069, 2.4507, 1.9068 ***(1061.70)***	3, 27, 5, 1.9070, 1.5655, 1.9069, 2.4507, 1.9068 ***(1056.80)***	3, 27, 5, 1.9070, 1.5655, 1.9069, 2.4508, 1.9068 ***(1054.50)***
(1.2, 1.3)	3, 27, 4.7781, 1.9070, 1.5652, 1.9067, 2.4547, 1.9068 ***(98.56)***	3, 27, 4.7288, 1.9070, 1.5651, 1.9069, 2.4562, 1.9068 ***(93.62)***	3, 27, 4.7128, 1.9070, 1.5650, 1.9069, 2.4568, 1.9068 ***(92.11)***	3, 27, 4.7049, 1.9070, 1.5650, 1.9069, 2.4571, 1.9068 ***(81.39)***
(1.4, 2.0)	3, 23, 3.7805, 1.9070, 1.4490, 1.9066, 2.7, 1.9068 ***(30.60)***	3, 23, 3.7813, 1.9070, 1.4490, 1.9066, 2.7, 1.9068 ***(29.46)***	3, 23, 3.7817, 1.9070, 1.4490, 1.9066, 2.7, 1.9068 ***(29.10)***	3, 23, 3.7819, 1.9070, 1.4490, 1.9066, 2.7, 1.9068 ***(28.93)***

The DS CV - ME chart under the error variance which is a linearly increasing function of the mean is also optimally designed to minimize EANOS$\left(\delta_{\min},\delta_{\max}\right)$ when the exact shift size is unknown. Here, $\left(\delta_{\min},\delta_{\max}\right) \in$ {(1.01, 1.05), (1.2, 1.3), (1.4, 2)} is considered. Table 4 shows the optimal parameters and corresponding EANOS $\left(\delta_{\min},\delta_{\max}\right)$ values for various values of θ, ω, ϕ, m and B. In Table 4, it is seen that an increase in θ decreases the sensitivity of the DS CV - ME chart, as EANOS$\left(\delta_{\min},\delta_{\max}\right)$ increases with θ. For instance, EANOS(1.01, 1.05) $\in$ {1047.30, 1052.93, 1063.58, 1073.93} for $\theta \in$ {0, 0.01, 0.03, 0.05} when $\omega = \phi = 0$, $m = B = 1$, γ_0 = 0.05 and n_0 = 5 (see Table 4). It is noticed in Table 4 that changes in ω and m do not affect EANOS$\left(\delta_{\min},\delta_{\max}\right)$. Therefore, taking multiple measurements per item ($m > 1$) does not improve the DS CV - ME chart's performance. Table 4 also shows that EANOS$\left(\delta_{\min},\delta_{\max}\right)$ increases with ϕ. For example, when $\theta = \omega = 0$, $m = B = 1$, γ_0 = 0.05 and n_0 = 5, EANOS(1.2, 1.3) $\in$ {89.28, 90.12, 92.60, 96.67} for $\phi \in$ {0, 0.1, 0.2, 0.3} (see Table 4). Additionally, in Table 4, it is found that the EANOS$\left(\delta_{\min},\delta_{\max}\right)$ performance of the DS CV - ME chart improves as B increases, i.e., the EANOS$\left(\delta_{\min},\delta_{\max}\right)$ value decreases as B increases. For example, EANOS(1.01, 1.05) $\in$ {98.56, 93.62, 92.11, 81.39}, for $B \in$ {1, 2, 3, 4} when θ = 0.05, m = 1, $\omega = \phi$ = 0.1, γ_0 = 0.05 and n_0 = 5 (see Table 4). In other words, an increase in the slope B of the measurement error model improves the sensitivity of the DS CV - ME chart.

8. A Real-world Example of Application

The working of the DS CV - ME chart is illustrated with a real-world example using an agricultural dataset from the NPK fertilizer company in Indonesia. The NPK fertilizer contains essential nutrients for plants, which include nitrogen (N), phosphorus (P) and potassium (K). In this section, the composition (in percentage) of phosphorus is the quality characteristic that will be monitored because phosphorus plays an important role for the photosynthesis and respiration process of plants. The fertilizer company adopts the CV type chart, instead of the common $\bar{X}$ chart to monitor the composition of phosphorus, as every batch or sample of the production process can contain various types of NPK fertilizers, such as “NPK 15-10-12”, “NPK 7-6-34” or “NPK 7-6-34+0.6B” fertilizer. Thus, the sample mean differs from one sample to the other but the process is considered as in-control if the ratio of the process standard deviation to the mean, called the CV, remains constant. To cater to this process monitoring situation, the CV type chart is employed.

Table 5: $\bar{\bar{X}}_i^*$, S_i^* and $\hat{\gamma}_i^*$ values for Phase-I dataset of composition (in percentage) of phosphorus in the production of NPK fertilizer

n_0 = 5			
Sample, i	$\bar{\bar{X}}_i^*$	S_i^*	$\hat{\gamma}_i^*$
1	9.3780	0.4454	0.0475
2	12.0300	0.6487	0.0539
3	9.9080	0.6120	0.0618
4	10.0260	0.4837	0.0482
5	10.0980	0.6231	0.0617
6	11.2960	0.6045	0.0535
7	11.3020	0.4930	0.0436
8	9.9020	0.6291	0.0635
9	10.1160	0.5180	0.0512
10	6.3740	0.2525	0.0396
11	6.7760	0.2984	0.0440
12	8.8000	0.6913	0.0786
13	9.7120	0.4157	0.0428
14	10.0260	0.6266	0.0625
15	9.8420	0.4980	0.0506
16	10.3440	0.2067	0.0200
17	10.0540	0.4950	0.0492
18	9.5320	0.4814	0.0505
19	9.2160	0.5680	0.0616
20	10.1500	0.7418	0.0731

Table 5 gives the sample mean $\left(\bar{\bar{X}}_i^*\right)$, standard deviation $\left(S_i^*\right)$ and CV $\left(\gamma_i^*\right)$, for 20 Phase-I samples, where i is the sample number. The linear covariate error model, based on the constant error variance approach is adopted, where θ = 0.01, η = 0.28, m = B = 1 and n_0 = 5 are used. By using the formula in Kang *et al*. (2007), the value of the in-control process CV in the presence of measurement errors, estimated from the Phase-I dataset in Table 5 is $\hat{\gamma}_0^* = \sqrt{\sum_{i=1}^{20}\left(n_0-1\right)\hat{\gamma}_i^{*2} \Big/ \sum_{i=1}^{20}\left(n_0-1\right)}$ = 0.0543. Figure 3 depicts the plotted Phase-I sample CVs,

$\hat{\gamma}_i^*$ (i = 1, 2, …, 20) on the Shewhart CV - ME chart, for the Phase-I dataset in Table 5. The LCL (= 0.0087) and UCL (= 0.1153) of this Phase-I Shewhart CV - ME chart are obtained by means of Equations (14) and (15) in Tran *et al*. (2019a). It can be deduced from Figure 3 that the Phase-I process CV is in-control, as all 20 $\hat{\gamma}_i^*$ values in Table 5 plot within the limits (LCL and UCL) of the chart. Therefore, $\hat{\gamma}_0^*$ (= 0.0543) is used in place of γ_0^* in Eqs. (21) and (22) to compute $\mu_0\left(\hat{\gamma}^* \mid \sum_{t=1}^{l} n_t\right)$ and $\sigma_0\left(\hat{\gamma}^* \mid \sum_{t=1}^{l} n_t\right)$, respectively, for l = 1 or 2, so that the limits of the DS CV - ME chart in Eqs. (20a) – (20d) can be calculated for Phase-II monitoring.

In Phase-II monitoring, the fertilizer company utilizes the DS CV - ME chart to monitor the process CV. Table 6 provides the Phase-II dataset for 15 sampling stages, which contains the sample means, $\bar{\bar{X}}_{li}^*$, standard deviations, S_{li}^*, and CVs, $\hat{\gamma}_{li}^*$, where l (= 1 or 2) denotes the inspection level and i (= 1, 2, …, 15) represents the sampling stage number. The optimal design of the DS CV - ME chart is made to minimize EANOS(1.2, 1.3), i.e., for shift sizes in the interval $(\delta_{\min}, \delta_{\max})$ = (1.2, 1.3), based on θ = 0.01, η = 0.28, m = B = 1 and n_0 = 5. With these parameter values, the optimal parameters $(n_1, n_2, ku_1^E, kl_1^E, wu^E, wl^E, ku_2^E, kl_2^E)$ = (3, 27, 4.7026, 1.9070, 1.5650, 1.9069, 2.4576, 1.9068) are obtained. By using Eqs. (20a) - (20d), the limits of the DS CV - ME chart, UCL_1^E, LCL_1^E, UWL^E, LWL^E, UCL_2^E and LCL_2^E are obtained as 0.1671, 0.000003, 0.0878, 0.000006, 0.0713 and 0.0403, respectively.

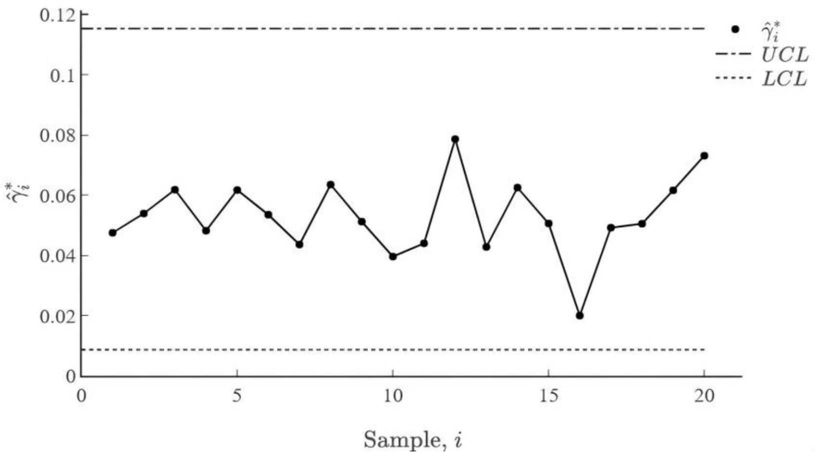

Figure 3: Shewhart CV - ME chart for Phase-I dataset of composition (in percentage) of phosphorus in the production of NPK fertilizer

The working of the DS CV – ME chart in Phase-II monitoring of the process CV is explained henceforth. The first sample of size n_1 = 3 observations is drawn and $\hat{\gamma}_{11}^*$ = 0.1402 is computed at inspection level 1 of sampling stage 1 (see Table 6). As $\hat{\gamma}_{11}^*$ = 0.1402 ∈ (UWL^E, UCL_1^E) = (0.0878, 0.1671), the second sample of size n_2 = 27 observations is drawn at inspection level 2 of the same sampling stage, where $\hat{\gamma}_1^{**}$ = 0.0611 is computed. As $\hat{\gamma}_1^{**}$ = 0.0611 ∈ (LCL_2^E, UCL_2^E) = (0.0403, 0.0713), the process is in-control at sampling stage 1. Taking samples and plotting the chart's statistics on the DS CV – ME chart continues in the same way until sampling stage 5 and it is found that sampling stages 1 – 5 are in-control. At sampling stage 6, $\hat{\gamma}^*_{16}$ = 0.0890 is obtained, where $\hat{\gamma}^*_{16} \in \left(UWL^E, UCL_1^E\right)$ = (0.0878, 0.1671), hence, the second sample of size n_2 = 27 observations is drawn at inspection level 2 of the said sampling stage. Then $\hat{\gamma}^{**}_6$ = 0.0283 is computed, which plots below LCL_2^E (= 0.0403). Thus, the process is out-of-control at sampling stage 6. Therefore, corrective actions ought to be made to get rid of the assignable cause that causes the process to shift. Figure 4 plots the Phase-II sample CVs using the dataset in Table 6.

Table 6: $\bar{\bar{X}}^*_{1i}$, S^*_{1i}, $\hat{\gamma}^*_{1i}$, $\bar{\bar{X}}^*_{2i}$, S^*_{2i}, $\hat{\gamma}^*_{2i}$ and $\hat{\gamma}^{**}_i$ values for Phase-II dataset of composition (in percentage) of phosphorus in the production of NPK fertilizer

Sampling stage, i	Inspection level 1 $n_1 = 3$			Inspection level 2 $n_2 = 27$			
	$\bar{\bar{X}}^*_{1i}$	S^*_{1i}	$\hat{\gamma}^*_{1i}$	$\bar{\bar{X}}^*_{2i}$	S^*_{2i}	$\hat{\gamma}^*_{2i}$	$\hat{\gamma}^{**}_i$
1	9.9667	1.3973	0.1402	8.7148	0.4370	0.0501	0.0611
2	5.9133	0.4801	0.0812				
3	6.5433	0.1464	0.0224				
4	7.0167	0.2570	0.0366				
5	7.2667	0.0635	0.0087				
6	7.9767	0.7101	0.0890	9.8285	0.8182	0.0832	0.0283
7	11.0100	0.0361	0.0033				
8	11.0800	0.0265	0.0024				
9	11.1367	0.0379	0.0034				
10	11.3267	0.1266	0.0112				
11	11.6433	0.1365	0.0117				
12	12.1133	0.1250	0.0103				
13	12.5200	0.0781	0.0062				
14	12.7667	0.0929	0.0073				
15	13.333	0.1930	0.0145				

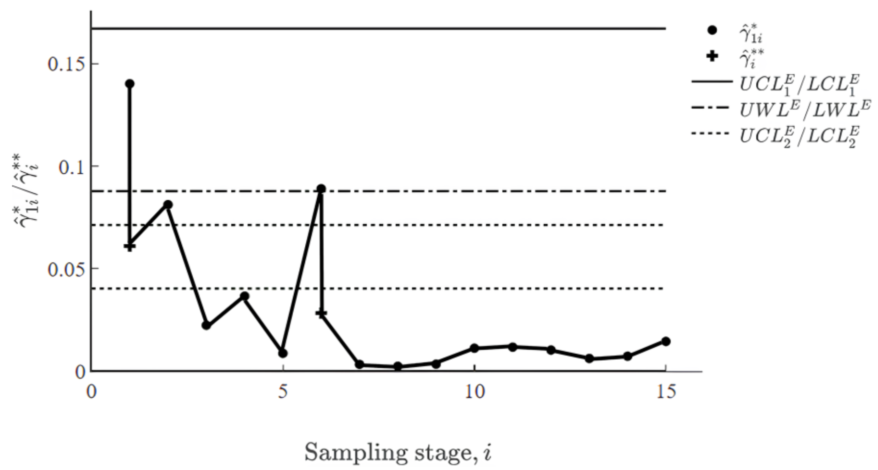

Figure 4: DS CV - ME chart for phase-II dataset of composition (in percentage) of phosphorus in the production of NPK fertilizer

9. Conclusion

In this study, the DS CV – ME chart's performance using the linear covariate error model when the error variance is constant and when it is a linearly increasing function of the mean is analyzed. To this end, the DS CV – ME chart is optimally designed for two different situations, i.e., when the exact shift size in the process CV can and cannot be specified, to minimize ANOS(δ) ($\delta > 1$) and EANOS$\left(\delta_{\min}, \delta_{\max}\right)$, respectively. It can be inferred that in both scenarios of constant error variance and error variance which is a linearly increasing function of the mean, an increase in θ affects the DS CV – ME chart's performance negatively because it slows down the chart's out-of-control detection speed. For the linear covariate error model with a constant error variance, changes in η does not change the DS CV – ME chart's performance. In like manner, under the linear covariate error model with an error variance which is a linearly increasing function of the mean, changes in the error component, ω, does not affect the chart's performance; but an increasing ϕ reduces the sensitivity of the chart designed to minimize ANOS(δ) ($\delta > 1$) and EANOS$\left(\delta_{\min}, \delta_{\max}\right)$. The findings show that under the constant error variance and the error variance which is a linearly increasing function of the mean, an increase in the coefficient B improves the DS CV – ME chart's performance, as ANOS(δ) (for $\delta > 1$) and EANOS$\left(\delta_{\min}, \delta_{\max}\right)$ decrease as B increases. Although taking multiple measurements per item (m) is a popular approach to reduce the negative effect of measurement errors, the numerical results show otherwise, as the ANOS(δ) (for $\delta > 1$) and EANOS$\left(\delta_{\min}, \delta_{\max}\right)$ performance of the DS CV – ME chart does not significantly improve as m increases, for the linear covariate error model based on the constant error variance and that based on an error variance which is a linearly increasing function of the mean.

In the current work, the implementation of the DS CV – ME chart is showcased through a real-world case study involving the NPK fertilizer dataset. The proposed chart can also be adapted for use in other industries, such as pharmaceuticals. A pharmaceutical company may produce various medicine dosages, leading to fluctuations in the sample means between samples, with the process standard deviation being proportional to the process mean. Additionally, operators may depend on weight gauges for dosage measurements, which can yield observed values that deviate from the true dosages.

In this study, the proposed DS CV - ME chart is evaluated only through statistical design. The economic design of the DS CV - ME chart can be proposed in a future study. The measurement error model considered in this study is the linear covariate error model. This study can be extended by studying the effect of measurement errors on the DS CV chart when the covariate error model is nonlinear. In addition, the proposed DS CV - ME chart is specifically developed for univariate process monitoring. An investigation as to how the DS chart performs in monitoring the multivariate CV when measurement errors exist can also be made in the future.

Appendix 1

This appendix illustrates how the term on the right-hand side of Eq. (12) is obtained. The left-hand side of Eq. (12) gives

$$\gamma^* = \frac{\sqrt{\dfrac{B^2 b^2 \sigma_0^2}{\mu_0^2} + \dfrac{\omega^2 \sigma_0^2}{\mu_0^2 m} + \dfrac{D\left(\mu_0 + a\sigma_0\right)}{\mu_0^2 m}}}{A + B\left(\mu_0 + a\sigma_0\right)/\mu_0} = \frac{\sqrt{B^2 b^2 \gamma_0^2 + \dfrac{\omega^2 \gamma_0^2}{m} + \dfrac{D\left(1 + a\gamma_0\right)}{\mu_0 m}}}{\theta + B\left(1 + a\gamma_0\right)}$$

$$= \frac{\sqrt{B^2 b^2 \gamma_0^2 + \frac{\omega^2 \gamma_0^2}{m} + \frac{\phi^2 \sigma_0^2 \left(1 + a\gamma_0\right)}{\mu_0{}^2 m}}}{\theta + B\left(1 + a\gamma_0\right)}$$

$$= \frac{\sqrt{B^2 b^2 \gamma_0^2 + \frac{\omega^2 \gamma_0^2}{m} + \frac{\phi^2 \gamma_0^2 \left(1 + a\gamma_0\right)}{m}}}{\theta + B\left(1 + a\gamma_0\right)}$$

$$= \frac{\gamma_0 \sqrt{B^2 b^2 + \frac{\omega^2}{m} + \frac{\phi^2 \left(1 + a\gamma_0\right)}{m}}}{\theta + B\left(1 + a\gamma_0\right)}.$$

Appendix 2

This appendix shows how the term on the right-hand side of Eq. (24) is obtained. The left-hand side of Eq. (24) gives

$$\begin{aligned} P_{\text{ooc1}}^{E} &= P\left(\hat{\gamma}_1^* \in R_3 \mid \gamma_+^*\right) \\ &= 1 - P\left(LCL_1^E \le \hat{\gamma}_1^* \le UCL_1^E \mid n_1, \gamma_+^*\right) \\ &= 1 - F_{\hat{\gamma}_1^*}\left(UCL_1^E \mid n_1, \gamma_+^*\right) + F_{\hat{\gamma}_1^*}\left(LCL_1^E \mid n_1, \gamma_+^*\right) \\ &= 1 - \left[1 - F_t\left(\frac{\sqrt{n_1}}{UCL_1^E} \mid n_1 - 1, \frac{\sqrt{n_1}}{\gamma_+^*}\right)\right] + \left[1 - F_t\left(\frac{\sqrt{n_1}}{LCL_1^E} \mid n_1 - 1, \frac{\sqrt{n_1}}{\gamma_+^*}\right)\right] \\ &= 1 - F_t\left(\frac{\sqrt{n_1}}{LCL_1^E} \mid n_1 - 1, \frac{\sqrt{n_1}}{\gamma_+^*}\right) + F_t\left(\frac{\sqrt{n_1}}{UCL_1^E} \mid n_1 - 1, \frac{\sqrt{n_1}}{\gamma_+^*}\right). \end{aligned}$$

Appendix 3

This appendix shows how the term on the right-hand side of Eq. (26) is obtained. The left-hand side of Eq. (26) gives

$$\begin{aligned} P\left(\hat{\gamma}_1^* \in R_2 \mid \gamma_+^*\right) &= P\left(LCL_1^E \le \hat{\gamma}_1^* \le LWL^E \mid n_1, \gamma_+^*\right) + P\left(UWL^E \le \hat{\gamma}_1^* \le UCL_1^E \mid n_1, \gamma_+^*\right) \\ &= P\left(\frac{\sqrt{n_1}}{LWL^E} \le \frac{\sqrt{n_1}}{\hat{\gamma}_1^*} \le \frac{\sqrt{n_1}}{LCL_1^E} \mid \gamma_+^*\right) + P\left(\frac{\sqrt{n_1}}{UCL_1^E} \le \frac{\sqrt{n_1}}{\hat{\gamma}_1^*} \le \frac{\sqrt{n_1}}{UWL^E} \mid \gamma_+^*\right) \\ &= P\left(\frac{\sqrt{n_1}}{LWL^E} \le u_1^* \le \frac{\sqrt{n_1}}{LCL_1^E} \mid \gamma_+^*\right) + P\left(\frac{\sqrt{n_1}}{UCL_1^E} \le u_1^* \le \frac{\sqrt{n_1}}{UWL^E} \mid \gamma_+^*\right) \\ &= \int_{\frac{\sqrt{n_1}}{LWL^E}}^{\frac{\sqrt{n_1}}{LCL_1^E}} f_t\left(u_1^* \mid n_1 - 1, \frac{\sqrt{n_1}}{\gamma_+^*}\right) du_1^* + \int_{\frac{\sqrt{n_1}}{UCL_1^E}}^{\frac{\sqrt{n_1}}{UWL^E}} f_t\left(u_1^* \mid n_1 - 1, \frac{\sqrt{n_1}}{\gamma_+^*}\right) du_1^*. \end{aligned}$$

Appendix 4

This appendix shows how the term on the right-hand side of Eq. (27) is obtained. The left-hand side of Eq. (27) gives

$$
\begin{aligned}
&P\left(\hat{\gamma}^{**} \in R_5 \mid n_1+n_2, \gamma_+^*\right) \\
&=1-P\left(\left(LCL_2^E\right)^2 \leq \frac{(n_1-1)\hat{\gamma}_1^{*2}+(n_2-1)\hat{\gamma}_2^{*2}}{(n_1-1)+(n_2-1)} \leq \left(UCL_2^E\right)^2 \mid n_1+n_2, \gamma_+^*\right) \\
&=1-P\left(\left[(n_1-1)+(n_2-1)\right]\left(LCL_2^E\right)^2 \leq (n_1-1)\hat{\gamma}_1^{*2}+(n_2-1)\hat{\gamma}_2^{*2} \leq \left[(n_1-1)+(n_2-1)\right]\left(UCL_2^E\right)^2 \mid n_1+n_2, \gamma_+^*\right) \\
&=1-P\left(\left[(n_1-1)+(n_2-1)\right]\left(LCL_2^E\right)^2-(n_1-1)\hat{\gamma}_1^{*2} \leq (n_2-1)\hat{\gamma}_2^{*2} \leq \left[(n_1-1)+(n_2-1)\right]\left(UCL_2^E\right)^2-(n_1-1)\hat{\gamma}_1^{*2} \mid n_1+n_2, \gamma_+^*\right) \\
&=1-P\left(\frac{\left[(n_1-1)+(n_2-1)\right]\left(LCL_2^E\right)^2-(n_1-1)\hat{\gamma}_1^{*2}}{n_2-1} \leq \hat{\gamma}_2^{*2} \leq \frac{\left[(n_1-1)+(n_2-1)\right]\left(UCL_2^E\right)^2-(n_1-1)\hat{\gamma}_1^{*2}}{n_2-1} \mid n_1+n_2, \gamma_+^*\right) \\
&=1-P\left(\left[\left(\frac{n_1-1}{n_2-1}+1\right)\left(LCL_2^E\right)^2-\left(\frac{n_1-1}{n_2-1}\right)\hat{\gamma}_1^{*2}\right] \leq \hat{\gamma}_2^{*2} \leq \left[\left(\frac{n_1-1}{n_2-1}+1\right)\left(UCL_2^E\right)^2-\left(\frac{n_1-1}{n_2-1}\right)\hat{\gamma}_1^{*2}\right] \mid n_1+n_2, \gamma_+^*\right).
\end{aligned}
\tag{A1}
$$

as $u_1^* = \dfrac{\sqrt{n_1}}{\hat{\gamma}_1^*}$, then $\hat{\gamma}_1^* = \dfrac{\sqrt{n_1}}{u_1^*}$. Therefore, Eq. (A1) can be written as

$$
\begin{aligned}
&P\left(\hat{\gamma}^{**} \in R_5 \mid n_1+n_2, \gamma_+^*\right) \\
&=1-P\left[\left(\frac{n_1-1}{n_2-1}+1\right)\left(LCL_2^E\right)^2-\frac{(n_1-1)n_1}{(n_2-1)u_1^{*2}} \leq \hat{\gamma}_2^{*2} \leq \left(\frac{n_1-1}{n_2-1}+1\right)\left(UCL_2^E\right)^2-\frac{(n_1-1)n_1}{(n_2-1)u_1^{*2}} \mid n_1+n_2, \gamma_+^*\right].
\end{aligned}
\tag{A2}
$$

In Section 5.1,

$$UCL_2^{E*} = \left(\frac{n_1-1}{n_2-1}+1\right)\left(UCL_2^E\right)^2-\frac{(n_1-1)n_1}{(n_2-1)u_1^{*2}}$$

and

$$LCL_2^{E*} = \left(\frac{n_1-1}{n_2-1}+1\right)\left(LCL_2^E\right)^2-\frac{(n_1-1)n_1}{(n_2-1)u_1^{*2}},$$

hence, Eq. (A2) can be simplified as

$$
\begin{aligned}
&P\left(\hat{\gamma}^{**} \in R_5 \mid n_1+n_2, \gamma_+^*\right) \\
&=1-P\left(LCL_2^{E*} \leq \hat{\gamma}_2^{*2} \leq UCL_2^{E*} \mid n_2, \gamma_+^*\right) \\
&=1-F_{\hat{\gamma}_2^{*2}}\left(UCL_2^{E*} \mid n_2, \gamma_+^*\right)+F_{\hat{\gamma}_2^{*2}}\left(LCL_2^{E*} \mid n_2, \gamma_+^*\right)
\end{aligned}
$$

$$=1-\left[1-F_F\left(\frac{n_2}{UCL_2^{E*}}\,|\,1,n_2-1,\frac{n_2}{\gamma_+^{*2}}\right)\right]+\left[1-F_F\left(\frac{n_2}{LCL_2^{E*}}\,|\,1,n_2-1,\frac{n_2}{\gamma_+^{*2}}\right)\right]$$

$$=F_F\left(\frac{n_2}{UCL_2^{E*}}\,|\,1,n_2-1,\frac{n_2}{\gamma_+^{*2}}\right)+\left[1-F_F\left(\frac{n_2}{LCL_2^{E*}}\,|\,1,n_2-1,\frac{n_2}{\gamma_+^{*2}}\right)\right].$$

Acknowledgments

This research was conducted when the corresponding author was spending his sabbatical leave at Estek Automation Sdn Bhd.

References

Abubakar S.S., Khoo M.B.C., Saha S., Umar A.A. & Yeong W.C. 2022. Run sum ratio chart when measurement errors are present. *Quality and Reliability Engineering International* **38**(8): 4049–4072.

Arshad A., Noor-ul-Amin M., Dogu E. & Hanif M. 2024. Performance of function-based AEWMA coefficient of variation control chart with measurement errors. *Communications in Statistics - Simulation and Computation* **53**(8): 3978–4000.

Calzada M.E., Scariano S.M. 2013. A synthetic control chart for the coefficient of variation. *Journal of Statistical Computation and Simulation* **83**(5): 853–867.

Castagliola P., Achouri A., Taleb H., Celano G. & Psarakis S. 2013. Monitoring the coefficient of variation using a variable sampling interval control chart. *Quality and Reliability Engineering International* **29**(8): 1135–1149.

Castagliola P., Achouri A., Taleb H., Celano G. & Psarakis S. 2015. Monitoring the coefficient of variation using a variable sample size control chart. *International Journal of Advanced Manufacturing Technology* **80**(9–12): 1561–1576.

Castagliola P., Celano G. & Psarakis S. 2011. Monitoring the coefficient of variation using EWMA charts. *Journal of Quality Technology* **43**(3): 249–265.

Cheng X.-B. & Wang F.-K. 2018a. The performance of EWMA median and CUSUM median control charts for a normal process with measurement errors. *Quality and Reliability Engineering International* **34**(2): 203–213.

Cheng X.-B. & Wang F.-K. 2018b. VSSI median control chart with estimated parameters and measurement errors. *Quality and Reliability Engineering International* **34**(5): 867–881.

Chong Z.L., Chew X., Khaw K.W., Teoh W.L. & Khoo M.B.C. 2025. Optimal design of the side sensitive modified group runs double sampling (SSMGRDS) $\bar{X}$ scheme with estimated process parameters. *Communications in Statistics – Simulation and Computation.* Advance online publication.

Diaz-Tufinio C.A., Gonzales-Covarrubias V. & Palma-Aguirre J.A. 2024. Pharmacological parameters and pharmacokinetic variability derived from bioequivalence trials in a Mexican population. *Clinical Pharmacology in Drug Development* **13**(1): 6–13.

Haizhen Z., Khoo M.B.C., Babatunde O.T. & Saha S. 2025. Effects of measurement errors on semicircle control chart. *Quality Engineering* **37**(3): 387–402.

Haq A., Brown J., Moltchanova E. & Al-Omari A.I. 2015. Effect of measurement error on exponentially weighted moving average control charts under ranked set sampling schemes. *Journal of Statistical Computation and Simulation* **85**(6): 1224–1246.

Haq A., Naz M. & Khoo M.B.C. 2024. Single and dual reference-free CUSCORE charts for detecting unknown patterned mean shifts. *Journal of Statistical Computation and Simulation* **94**(3): 484–498.

Hassani Z., Amiri A. & Castagliola P. 2021. Variable sample size of exponentially weighted moving average chart with measurement errors. *Scientia Iranica* **28**(4): 2386–2399.

Hong E.P., Kang C.W., Kang H.W. & Baek J.W. 2008. Development of CV control chart using EWMA technique. *Journal of Society of Korea Industrial and Systems Engineering* **31**(4): 114–120.

Hu X., Castagliola P., Sun J. & Khoo M.B.C. 2015. The effect of measurement errors on the synthetic $\bar{x}$ chart. *Quality and Reliability Engineering International* **31**(8): 1769–1778.

Hu X., Castagliola P., Sun J. & Khoo M.B.C. 2016. The performance of variable sample size $\bar{x}$ chart with measurement errors. *Quality and Reliability Engineering International* **32**(3): 969–983.

Jin J., Yan H. & Zhao Q. 2022. Convergence spatial measurement of economic growth based on big data. *Mobile Information Systems* **2022**(1): 6230817.

Kang C.W., Lee M.S., Seong Y.J. & Hawkins D.M. 2007. A control chart for the coefficient of variation. *Journal of Quality Technology* **39**(2): 151–158.

Khaw K.W., Khoo M.B.C., Yeong W.C. & Wu Z. 2017. Monitoring the coefficient of variation using a variable sample size and sampling interval control chart. *Communications in Statistics - Simulation and Computation* **46**(7): 5772–5794.
Lau W.K., Chong Z.L. & Ng P.S. 2018. One-sided variable sampling interval control chart for monitoring the coefficient of variation. *Proceedings of the 2018 4th International Conference on Electrical, Electronics and System Engineering* **2**: 40–43.
Lee M.H., Khoo M.B.C., Chew X. & Then P.H.H. 2020. Effect of measurement errors on the performance of coefficient of variation chart with short production runs. *IEEE Access* **8**: 72216–72228.
Lee P.H. 2013. Joint statistical design of $\bar{X}$ and s charts with combined double sampling and variable sampling interval. *European Journal of Operational Research* **225**(2): 285–297.
Lee P.H., Torng C.C., Jhong H.R. & Chou C.Y. 2021. Monitoring the coefficient of variation using a double-sampling control chart. *Communications in Statistics - Simulation and Computation* **52**(10): 4849–4863.
Lim S.L., Yeong W.C., Chong Z.L., Gan C.P. & Khoo M.B.C. 2024. A variable sample size side-sensitive synthetic coefficient of variation chart. *Transactions of the Institute of Measurement and Control* **46**(9): 1694–1712.
Linna K.W. & Woodall W.H. 2001. Effect of measurement error on Shewhart control charts. *Journal of Quality Technology* **33**(2): 213–222.
Maravelakis P. Panaretos J.P. & Psarakis S. 2004. EWMA chart and measurement error. *Journal of Applied Statistics* **31**(4): 445–455.
Mehmood R., Mpungu K., Ali I., Zaman B., Qureshi F.H. & Khan N. 2023. A new approach for designing the Shewhart-type control charts with generalized sensitizing rules. *Computers and Industrial Engineering* **182**: 109379.
Mim F.N., Khoo M.B.C., Saha S. & Khaw K.W. 2023. A side-sensitive group runs median control chart with measurement errors. *Communications in Statistics - Simulation and Computation* **52**(4): 1660–1678.
Montgomery D.C. & Runger G.C. 1993. Gauge capability and designed experiments. Part I: Basic methods. *Quality Engineering* **6**(1): 115–135.
Munir T., Hu X., Kauppila O. & Bergquist B. 2023. Effect of measurement uncertainty on combined quality control charts. *Computers & Industrial Engineering* **175**: 108900.
Nguyen H.D. & Tran K.P. 2020. Effect of the measurement errors on two one-sided Shewhart control charts for monitoring the ratio of two normal variables. *Quality and Reliability Engineering International* **36**(5): 1731–1750.
Nguyen H.D., Nguyen Q.T., Tran K.P. & Ho D.P. 2019. On the performance of VSI Shewhart control chart for monitoring the coefficient of variation in the presence of measurement errors. *The International Journal of Advanced Manufacturing Technology* **104**(1–4): 211–243.
Nguyen H.D., Tran K.P., Celano G., Maravelakis P.E. & Castagliola P. 2020. On the effect of the measurement error on Shewhart t and EWMA t control charts. *The International Journal of Advanced Manufacturing Technology* **107**(9–10): 4317–4332.
Pélabon C., Hilde C.H., Einum S. & Gamelon M. 2020. On the use of the coefficient of variation to quantify and compare trait variation. *Evolution Letters* **4**(3): 180–188.
Saadatmellia A., Seif A. & Moghadam M.B. 2023. Optimization of design parameters for $\bar{X}$ control charts with independent multiple assignable causes based on continuous flow processes. *Fluctuation and Noise Letters* **22**(6): 2350047.
Sharafi S., Khanbeygi P., Maleki M.R. & Salmasnia A. 2024. A double-sampling approach for multivariate control charting using multiple measurement strategy and simulation. *International Journal of Management and Decision Making* **23**(2): 137–153.
Saha S., Khoo M.B.C., Castagliola P. & Haq A. 2021. Side-sensitive modified group runs charts with and without measurement errors for monitoring the coefficient of variation. *Quality and Reliability Engineering International* **37**(2): 598–617.
Saha S., Khoo M.B.C., Chatterjee K. & Godase D.G. 2026. Multivariate triple sampling Hotelling's T^2 control chart. *Quality Technology & Quantitative Management* **23**(1): 129–143.
Saha S., Khoo M.B.C., Mim F.N., Chatterjee K. & Yeong W.C. 2024. Variable parameters t chart: An application in automobile engine piston rings manufacturing process. *International Journal of Reliability, Quality and Safety Engineering* **31**(6): 2450037.
Santhanasamy D.K. & Abdul-Rahman A. 2022. Robustification of Shewhart control chart by median based estimators: A study on Malaysia stock data. *Journal of Quality Measurement and Analysis* **18**(1): 13–26.
Shafie S.N.A.M., Shaadan N., Hamzah F.M. & Mansor M.M. 2025. A comparison of various residual-based control charts for detecting and monitoring abnormal river water levels. *Journal of Quality Measurement and Analysis* **21**(1): 253–265.
Sparks R.S. 2000. CUSUM charts for signalling varying location shifts. *Journal of Quality Technology* **32**(2): 157–171.

Teoh J.W., Teoh W.L., Khoo M.B.C., Tran K.P. & Lee M.H. 2025a. An integrated optimal-GICP design for the SPRT control chart with estimated process parameters based on the average number of observations to signal. *Quality Technology & Quantitative Management* **22**(1): 84–104.

Teoh J.W., Teoh W.L., Hu X., Tran K.P. & Godase D.G. 2025b. A new omnibus SPRT chart for monitoring process mean and variability based on the average number of observations to signal. *Journal of Statistical Computation and Simulation* **95**(1): 49–69.

Teoh W.L., Liow K.L., Khoo M.B.C., Yeong W.C. & Teh S.Y. 2014. A comparison between the performance of double sampling $\bar{X}$ and variable sample size $\bar{X}$ charts. *Journal of Quality Measurement and Analysis* **10**(2): 15–31.

Tran K.P., Heuchenne C. & Balakrishnan N. 2019a. On the performance of coefficient of variation charts in the presence of measurement errors. *Quality and Reliability Engineering International* **35**(1): 329–350.

Tran P.H., Tran K.P. & Rakitzis A. 2019b. A synthetic median control chart for monitoring the process mean with measurement errors. *Quality and Reliability Engineering International* **35**(4): 1100–1116.

Whelen T. & Siqueira P. 2018. Coefficient of variation for use in crop area classification across multiple climates. *International Journal of Applied Earth Observation and Geoinformation* **67**: 114–122.

Wu Z., Yang M., Jiang W. & Khoo M.B.C. 2008. Optimization designs of the combined Shewhart-CUSUM control charts. *Computational Statistics and Data Analysis* **53**(2): 496–506.

Xie F., Castagliola P., Tang A., Hu X. & Sun J. 2024. The performance of the one-sided truncated exponentially weighted moving average $\bar{X}$ control chart in the presence of measurement errors. *Journal of Statistical Computation and Simulation* **94**(10): 2089–2113.

Yeong W.C., Khoo M.B.C., Lim S.L. & Lee M.H. 2017a. A direct procedure for monitoring the coefficient of variation using a variable sample size scheme. *Communications in Statistics - Simulation and Computation*, **46**(6): 4210–4225.

Yeong W.C., Khoo M.B.C., Lim S.L. & Teoh W.L. 2017b. The coefficient of variation chart with measurement error. *Quality Technology & Quantitative Management* **14**(4): 353–377.

Yeong W.C., Lim S.L., Khoo M.B.C. & Castagliola P. 2018. Monitoring the coefficient of variation using a variable parameters chart. *Quality Engineering* **30**(2): 212–235.

Zhang J., Li Z., Chen B. & Wang Z. 2014. A new exponentially weighted moving average control chart for monitoring the coefficient of variation. *Computers and Industrial Engineering* **78:** 205–212.

School of Mathematical Sciences
Universiti Sains Malaysia
11800 Minden
Penang, MALAYSIA
*E-mail: alifian.nuriman@student.usm.my, mkbc@usm.my**

Department of Business Statistics
Institut Teknologi Sepuluh Nopember
Surabaya, INDONESIA
E-mail: alifian.nuriman@student.usm.my

Department of Mathematics
International University of Business Agriculture and Technology
1230 Dhaka, BANGLADESH
E-mail: sajal.saha@iubat.edu

Department of Electronic Engineering
Faculty of Engineering and Green Technology
Universiti Tunku Abdul Rahman
31900 Kampar
Perak, MALAYSIA
E-mail: chongzl@utar.edu.my

Estek Automation Sdn Bhd
No. 53, Jalan Sungai Tiram 2
Nyaman Mutiara Light Industrial Park 2, Sungai Tiram
11900 Bayan Lepas,
Penang, MALAYSIA
E-mail: shanyu.chua@estechs.com

Received: 1 July 2025
Accepted: 8 September 2025

*Corresponding author